INFLUENCES OF COMBINATORIALLY SELECTED PEPTIDES ON INHIBITION OF *GIBBERELLA ZEAE* SPORE GERMINATION AND CYTOLOGICAL MODIFICATION OF EMERGING GERM-TUBES

A Thesis

presented to

the Faculty of the Graduate School

at the University of Missouri-Columbia

In Partial Fulfillment

of the Requirements for the Degree

Master of Science

---

by

NATHAN WILSON GROSS

Professor James T English, Thesis Supervisor

JULY 2012

The undersigned, appointed by the dean of the Graduate School, have examined the thesis entitled

Influences of Combinatorially Selected Peptides on Inhibition of Gibberella zeae Spore Germination and Cytological Modification of Emerging Germ-Tubes

presented by Nathan W Gross,

a candidate for the degree of master of science,

and hereby certify that, in their opinion, it is worthy of acceptance.

Professor James T English

Professor James E Schoelz

Professor Francis J Schmidt

ACKNOWLEDGMENTS

I would like to thank my advisor, Professor Jim English, for the help, encouragement, and patience he generously gave throughout my student experience. I would also like to thank my committee, consisting of Professors Jim Schoelz and Frank Schmidt, for their technical guidance and critical eye. Additionally, much of what I have learned in regards to laboratory skill can be attributed to Dr Zhiwei Fang.

I would like to thank Professor Frances Trail from Michigan State University for supplying *Gibberella zeae* PH-1 and for guiding me through the culturing of perithecia.

My work relied heavily on the University of Missouri Molecular Cytology and DNA-Sequencing core facilities. I would like to thank the university for providing these tools and their staff for excellent work and technical assistance.

I would like to thank Daniel F Millikan III for the endowment he left to fund plant pathology graduate studies. The Millikan Fund paid most of my academic fees, travel expenses, and stipend.

Lastly, I would like to thank my friends and family for their patience and support through my studies at the University of Missouri and through life, in general.

TABLE OF CONTENTS

LIST OF FIGURES

LIST OF TABLES

CHAPTER ONE

INTRODUCTION

Head Blight of Wheat. Head blight, alternatively known as scab, is an economically important disease of wheat, barley, and other cereal crops worldwide. In the United States, the disease is primarily caused by the ascomycete, *Gibberella zeae* (Schweinitz) Petch (anamorph *Fusarium graminearum* (Schwabe))(15). Head blight was first identified in England in 1884, and it has spread across the globe with head-blight epidemics occurring periodically throughout all wheat-growing areas (15).

Head blight not only limits grain yield but also reduces grain quality that results from accumulation of mycotoxins produced by the pathogen (15). The most significant of the mycotoxins is deoxynivalinol (DON), a protein-synthesis inhibitor (2,15). Concentrations of DON in harvested grain above defined thresholds reduce the marketability of infected grain (2,15).

Head blight is first evident when infected florets of the wheat head, the plant's inflorescence, become water-soaked. Quickly, infected florets become chlorotic and then necrotic (Fig. 1A). Grain harvested from infected plants appears shriveled and shrunken, and signs of the pathogen may be evident, including aerial mycelium, macroconidia, and perithecia (15,16).

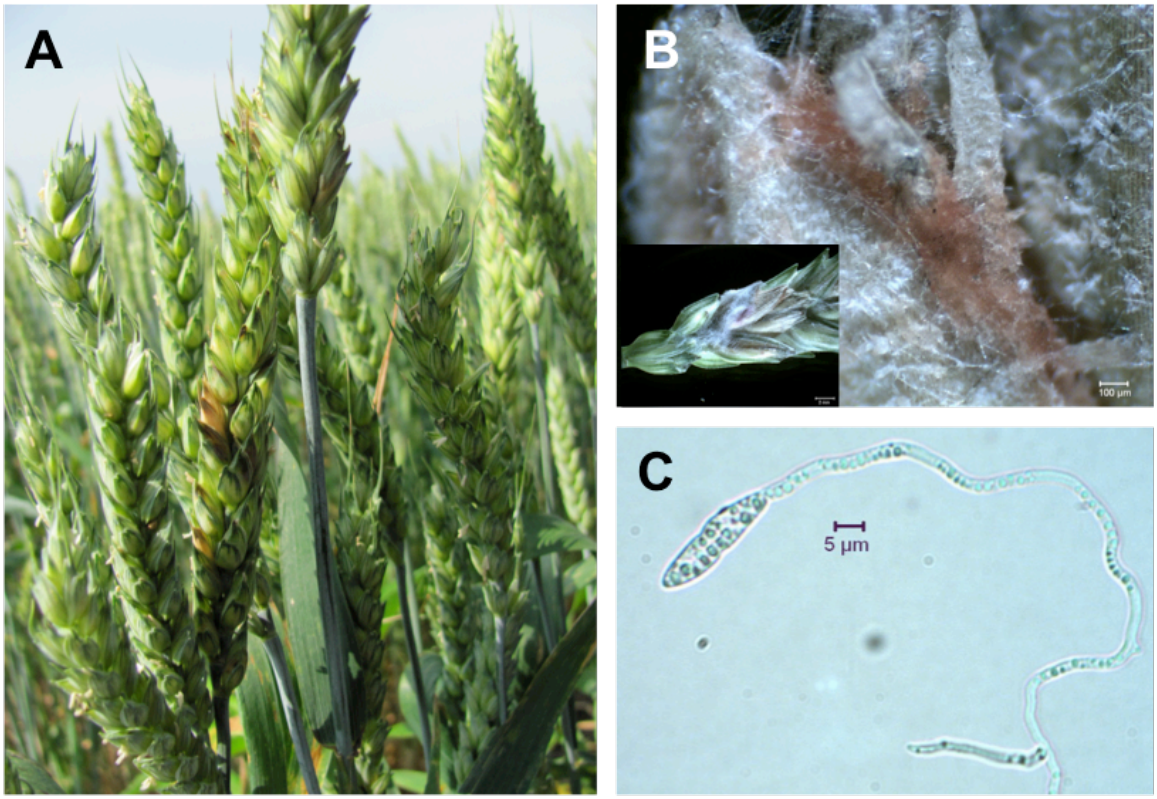

Fig. 1: Wheat with head-blight symptoms **A**. Aerial mycelium of *G. zeae* colonizing the surfaces of florets **B** and inset. Germinated *Gibberella zeae* ascospore **C**.

Disease cycle. Initial infection of wheat by *G. zeae* occurs in the springtime during anthesis when the floret's palea and lemma open to allow anthers to emerge and disperse pollen. Coincidently at this time, ascospores are forcibly discharged from perithecia present on crop residue from the previous growing season (1,15,16,27). Ascospores are ejected from perithecia above the crop canopy and can be carried long distances by wind movement (1,13,15).

Ascospores that land on tissues exposed during anthesis germinate to begin the infection process (Fig. 1C). Under favorable conditions of high humidity, free moisture, and cool temperatures, the hyphae produced after ascospore germination may colonize the exterior, then interior epidermal cells, of the palea and lemma (Fig. 1B and inset)(1,2,9,10,15,16,17,). From there, the pathogen can colonize reproductive tissues (15,16). From colonized floral tissue, hyphae progressively colonize the inflorescence vasculature, termed the rachis. From the rachis, hyphae colonize other florets above and below the initial infection point (15,16). From a colonized inflorescence, *G. zeae* may colonize other tissues of the plant, including the stems and leaves.

Both sexual and asexual reproduction of *G. zeae* occurs in colonized tissues during plant senescence and after plant death (15,16,27). Asexually produced macroconidia are developed from a sporodochium and can be dispersed locally by rain splash, wind, insect, animal and mechanical transport (13,15,17). The contribution of macroconidia to head blight development is minimal because they are formed late in the wheat-growing season (15). Sexual reproduction results in perithecia that contain ascospores (15,16,27). Perithecia are composed of thick melanized hyphae that protect

developing ascospores from exposure to ultraviolet radiation and cold temperatures during fall and winter months (16,27).

Perithecia in wheat stems and other crop residue mature the following spring. At that time, ascospores are produced and discharged to initiate infection of flowering wheat plants. As *G. zeae* is pathogenic on other common rotational crop plants such as corn, residue from those crops may also contribute inoculum to initiate new wheat infections (10,16,27).

Head blight management. Head blight is managed by application of protective fungicides and host-plant resistance. These measures may be implemented individually or in combination (16). Fungicide application over large wheat production fields can be expensive, and the timing of applications is difficult to predict. Recently, computer models have been developed to assist wheat producers with planning of fungicide applications (9,10,15).

The most reliable disease control measure is the use of resistant wheat cultivars. Host resistance to head blight is not manifested in a gene-for-gene manner because no fungal races of *G. zeae* have been identified. (14,16). Head-blight resistance is, instead, manifested as quantitative-trait (15). Several partially resistant varieties of wheat are on the market (15). Two forms of resistance to head blight are most recognized. Type I resistance refers to protection of wheat heads against initial infection by *G. zeae* (15). Type II resistance refers to the restricted growth of *G. zeae* from an initial infection site to surrounding tissues (15). Other resistance types have been described and are based on reductions of DON accumulation in colonized grain and limitations in yield loss (2,15).

Biology of *Gibberella zeae* growth and development. *Gibberella zeae* ascospores consist of two to four cells. Most ascospores germinate from only one of the two apical cells, and germination rarely occurs from an intercalary ascospore cell (16,24). Macroconidia germinate in a similar fashion (16,17,24). The germ-tube produced during germination elongates to produce a hypha. Germ-tube and hyphal elongation are highly polarized processes based on controlled extension of the apical cell at a single point (17,18,24).

Polarized growth leads to the formation of hyphae with a generally uniform diameter (17,18). Over time, lateral hyphal branches emerge and establish their own polar identity (17,18). Ultimately, a network of hyphae, the mycelium, develops to locate and extract nutrients from the surrounding environment.

Germ-tube and hyphal elongation in *G. zeae* and other filamentous fungi is directed by the Spitzenkörper that acts as a vesicle organization center (5,6,17,18). By microscopic observation, the Spitzenkörper is usually seen as a dense, dark spot located adjacent to the polar tip of the hyphal apex. Vesicles within the Spitzenkörper are derived from the Golgi body and arrive by transport along microtubule filaments. From the Spitzenkörper, vesicles are transported via actin filaments to the plasma membrane at the polar tip of the cell (5,6,17,18,29). There, vesicles fuse with the plasma membrane, expanding the surface area of the membrane while also delivering cell-wall precursors. Trans-membrane proteins, including chitin and glucan synthases that are carried by vesicles are incorporated into the expanding plasma membrane (5,6,17,18,25,28).

As the plasma membrane surface area increases, the plasma membrane is also internalized subapically by endocytosis (17,18,21,30). During endocytosis, the plasma

membrane with associated proteins and molecules derived from the external environment is pinched off to form small vesicles known as endosomes (26). As they are produced, endosomes are sorted and transported along microtubule filaments to either the Spitzenkörper or for recycling to vacuoles where their contents are stored or degraded. Endocytosis is an important process for the internalization of nutritional and signaling molecules such as amino acids and peptides (21,26,30).

Proteins associated with plasma membranes of germ-tube or hyphal cells are not spatially homogeneous but occur in unevenly distributed aggregates (8,21). Penalva (21) and Cheng et al. (8) have suggested that the distribution of sterol rich domains (SRDs) within the plasma membrane influence the aggregation of membrane associated proteins. In fungi, the most abundant plasma membrane sterol is ergosterol (8). In addition to influences on protein aggregation, SRDs have been shown to affect polarized hyphal growth by anchoring cytoskeletal filaments involved in vesicle trafficking (23). Rittenour et al. (23) also established that SRDs were involved with successful host infection by the pathogen. Sterol rich domains within the hyphal plasma membrane are typically localized to polar tip of the apical cell, but SRDs are also observed at points of septum formation (22).

The cell wall is synthesized at the germ-tube or hyphal apex in conjunction with plasma membrane formation (5,6). Cell wall synthesis also occurs in conjunction with the formation of hyphal septation (5,6). When synthesized, the cell wall is initially thin and consists primarily of chitin chains, composed of β1,4-linked *N*-acetylglucosamine subunits that form strong hydrogen bonds among adjacent chains to develop fibrils. These chitin fibrils, and other cell-wall polysaccharides such as β-glucans form a thicker,

subapical cell wall consisting of several layers (5,6). The mature cell wall of filamentous fungi consists of 10 to 20 % chitin (5). Glycoprotein components, anchored to the plasma membrane, are also intercalated within the cell wall (5,6). The increasing thickness and subsequent rigidity of subapical germ-tube cells provide structural support (5,6). The cell wall is the initial region of physical contact between a fungal pathogen and a host plant; as such it is an important factor for successful host infection (5,6).

Antimicrobial peptides for plant protection. Peptides smaller than 40 amino acids have been proposed as a strategy for plant protection (20). The most common reasons are to reduce the amount of pesticides used in crop production fields and as a method to reduce the occurrences of pathogen resistance to pesticides (20).

Many of the studied antimicrobial peptides have been derived from natural sources such as from plants, microorganisms, and animals (20). Many of these peptides are known to interact with cell membranes and induce lysis, however other modes of action have been found (20). Often, antimicrobial peptides of natural origin must be modified in amino acid sequence, either to increase their efficiency or decrease cytotoxicity in non-target organisms, such as plants or animals (20).

Although antimicrobial peptides have been identified from these natural sources, other methods are commonly used. One is through the use of synthetic peptide libraries or collections (20,22,26). Two types of synthetic peptide libraries are commonly used. A nondefined synthetic peptide library consist of peptides of a specific size that contain all possible combinations of their amino acid sequence (20). Peptides from these libraries are either incubated in vitro with a target pathogen to determine antimicrobial property or with a known, specific target upon or within a target pathogen (20).

Another type of synthetic peptide library is the defined library. These are libraries in which a specific amino acid sequence of known biological function is included in each member library (20). For example, if a peptide amino acid sequence is known to bind to a specific component of a microorganism, such as a plasma membrane or cell wall, each peptide derivative would contain that specific sequence along with a random sequence component.

Antimicrobial peptides have also been identified from specific regions of proteins, synthesized and assayed for effect (20). For example, if a short amino acid sequence is known to have biological activity and the remaining protein domains do not, a library can be constructed based on the active protein site.

Another, more recent strategy for the discovery of antimicrobial peptides is the use of in silico strategies (20). In this technique, antimicrobial properties of peptides are based on computer simulations with defined rules, termed grammar rules, which determine peptide efficiency by the topology of virtual target pathogen proteins (20).

Lastly, antimicrobial peptides can be identified by biotechnological methods (20). One method, phage display, was the method used in this study and will be discussed in detail below.

Phage display selection of fungal inhibitory peptides. Peptides with binding affinity for germinated ascospores can be identified from combinatorial phage-display libraries. Two types of phage-display peptide libraries have been utilized to identify fungal inhibitory peptides. One phage-display library, f8, consists of the fd bacteriophage strain modified to express a random 8-amino-acid peptide at the N-terminus of the major coat protein VIII (22,26). In an f8 library, each phage expresses a single peptide variant on

each of about 4,000 copies of coat protein VIII (26). The f8 library contained 1.5 x 10^9 peptide variants.

A second combinatorial library, Ph.D.-12, consistes of M13 filamentous phage and expresses a 12-amino-acid peptide fused to the N-terminus of the minor coat protein III. Each phage in this library displays one peptide variant on each of five copies of coat protein III, and a typical library contains 4.1 x 10^{15} possible random 12-a.a. sequences (12).

These two phage display peptide libraries have been screened to identify peptides that inhibit the growth or proper development of fungal and oomycecious plant pathogens. For example, Bishop-Hurley, et al (3) selected peptides with binding affinity for zoospores of the biotrophic oomycete, *Phytophthora capsici.* Several of these peptides were found to induce premature zoospore encystment. When the peptides were expressed in tomato hairy-roots, they induced zoospore encystment at a distance from the root surface and subsequently reduced root infection (3,11). More recently, Fang, et al (12) selected peptides that bind to germ-tubes and urediniospores produced by *Phakopsora pachyrhizi,* the fungal pathogen that causes Asian soybean rust (12). Several of these peptides were shown to delay infection of soybean leaves when urediniospores and peptides were coinoculated onto soybean leaves.

Selection of peptides that inhibit *G. zeae* growth and development. The successes of Bishop-Hurley (3,4) and Fang (11,12) in identifying inhibitory peptides from combinatorial phage-display libraries suggests *G. zeae* growth and development may also be inhibited by combinatorially selected peptides. Therefore, the goal of this study was to identify peptides from phage-display peptide libraries with affinity for

germinating spores of *G. zeae*. The resulting collection of phage-display peptides was then assessed for their ability to interrupt growth and development of *G. zeae* macroconidia through in vitro assays. Upon identification, macroconidium growth inhibitory peptides were tested for efficacy against ascospores as they are primary inoculum for head blight infections. Peptides, derived from inhibitory phage-display peptide clones were chemically synthesized and a study of concentration dependence was carried out. Lastly, after an analysis of the gross, morphological alterations of peptide exposed ascospores, fluorescent probes were utilized to observe specific cytological modifications induced by *G. zeae* growth inhibitory peptides.

LITERATURE CITED

1. Beyer, M. and Verreet, J-A. 2005. Germination of *Gibberella zeae* ascospores as affected by age of spores after discharge and environmental factors. Eur. J. Plant Pathol. 111:381-389.
2. Beyer, M., Verreet, J-A., and Ragab, W. S. M. 2005. Effect of relative humidity on germination of ascospores and macroconidia of *Gibberella zeae* and deoxynivalenol production. Int. J. Food. Microbiol. 98:233-240.
3. Bishop-Hurley, S. L., Mounter, S. A., Laskey, J., Morris, R. O., Elder, J, Roop, P., Rouse, C., Schmidt, F. J., and English, J. T. 2002. Phage-displayed peptides as developmental agonists for *Phytophthora capsici* zoospores. App. Environ. Mircobiol. 68:3315-3320.
4. Bishop-Hurley, S. L., Schmidt, F. J., Erwin, A. L., Smith, A. L. 2005. Peptides selected for binding to a virulent strain of *Haemophilus influenzae* by phage display are bactericidal. Antimicrob. Agents Chemother. 49:2972-2978.
5. Bowman, S. M. and Free, S. J. 2006. The structure and synthesis of the fungal cell wall. BioEssays 28:799-808.
6. Cabib, E. The synthesis and degradation of chitin. Adv. Enzymol. 59:59-101.
7. Cheng, J., Park, T-S., Fischl, A. S., and Ye, X. S. 2001. Cell cycle progression and cell polarity require sphingolipid biosynthesis in *Aspergillus nidulans*. Mol. Cell Biol. 21:6198-6209.
8. Correll, J. C., Klittich, C. J. R., and Leslie, J. F. 1987. Nitrate nonutilizing mutants for *Fusarium oxysporum* and their use in vegetative compatibility tests. Phytopathology 77:1640-1646.

9. De Wolf, E. D., Madden, L. V., and Lipps, P. E. 2003. Risk assessment models for wheat Fusarium head blight epidemics based on within-season weather data. Phytopathology 93:428-435.
10. De Wolf, E. D. and Isard, S. A. 2007. Disease cycle approach to plant disease prediction. Annu. Rev. Phytopathol. 45:1-18.
11. Fang, Z. D., Laskey, J. G., Huang, S., Bilyeu, K. D., Morris, R. O., Schmidt, F. J., and English, J. T. 2006. Combinatorially selected defense peptides protect plant roots from pathogen infection. Proc. Natl. Acad. Sci. USA 103:18444-18449.
12. Fang, Z. D., Marois, J. J., Stacey, G., Schoelz, J. E., English, J. T., and Schmidt, F. J. 2010. Combinatorially selected peptides for protection of soybean against *Phakopsora pachyrhizi*. Phytopathology 100:1111-1117.
13. Fernando, W. G. D., Miller, J. D., Seaman, W. L., Seifert, K., and Paulitz, T. C. 2000. Daily and seasonal dynamics of airborne spores of *Fusarium graminearum* and other *Fusarium* species sampled over wheat plots. Can. J. Bot. 78:497-505.
14. Flor, H. H. 1942. Inheritance of pathogenicity in *Melampsora lini*. Phytopathology 32: 653-669.
15. Goswami, R. S., and Kistler, H. C. 2004. Pathogen profile: Heading for disaster: *Fusarium graminearum* on cereal crops. Mol. Plant Pathol. 5:515-525.
16. Guenther, J. C. and Trail, F. 2005. The development and differentiation of *Gibberella zeae* (anamorph: *Fusarium graminearum*) during colonization of wheat. Mycologia 97:229-237.
17. Harris, S. D. 2005. Morphogenesis in germinating *Fusarium graminearum* macroconidia. Mycologia 97:880-887.

18. Harris, S. D., Hofmann, A. F., Tedford, H. W., and Lee, M. P. 1999. Identification and characterization of genes required for hyphal morphogenesis in the filamentous fungus *Aspergillus nidulans.* Genetics. 151:1015-1025.

19. Hill, D. F., Pertersen, G. B. 1982. Nucleotide sequence of bacteriophage f1 DNA. J. Virol. 44:32-46.

20. Marcos, J. F., Muñuz, A., Pérez-Payá, E., Misra, S., and López-García, B. 2008. Identification and rational design of novel antimicrobial peptides for plant protection. Annu. Rev. Phytopathol. 46:273-301.

21. Peñalva, M. A. 2005. Tracing the endocytic pathway of *Aspergillus nidulans* with FM4-64. Fungal. Genet. Biol. 42:963-975.

22. Petrenko, V. A., Smith, G. P., Gong, X. and Quinn, T. 1996. A library of organic landscapes on filamentous phage. Protein Eng. 9:797-801.

23. Rittenour, W. R., Chen, M., Cahoon, E. B., and Harris, S. D. 2011. Control of glucosylceramide production and morphogenesis by the Bar1 Ceramide Synthase in *Fusarium graminearum.* PLoS One. 6:e19385.

24. Seong, K-Y., Zhao, X., Xu, J-R., Güldener, U., and Kistler, H. C. 2008. Conidial germinaiton in the filamentous fungus *Fusarium graminearum.* Fungal Genet. Biol. 45:389-399.

25. Smith, G. P. and Petrenko, V. A. 1997. Phage Display. Chem. Rev. 97:391-410.

26. Steinberg, G. 2007. On the move: endosomes in fungal growth and pathogenicity. Nature Rev. Microbiol. 5:309-316.

27. Trail, F., Common, R. 2000. Perithecial development by *Gibberella zeae:* a light microscopy study. Mycologia 92:130–138.

28. Upadhyay, S. and Shaw, B. D. 2008. The role of actin, fimbrin and endocytosis in growth of hyphae in *Aspergillus nidulans.* Mol. Microbiol. 68:690-705.

29. Veses, V., Richards, A., Gow, A. R. 2008. Vacuoles and fungal biology. Curr. Opin. Microbiol. 11:503-510.

30. Xu, X-M., Monger, W., Ritieni, A., and Nicholson, P. 2007. Effect of temperature and duration of wetness during initial infection periods on disease development, fungal biomass and mycotoxin concentrations on wheat inoculated with single, or combinations of, *Fusarium* species. Plant Pathol. 56:943-956.

31. Yu, J. and Smith, G. P. 1996. Affinity maturation of phage-displayed peptide ligands. Methods Enzymol. 267:3-27.

CHAPTER TWO

INFLUENCE OF COMBINATORIALLY SELECTED PEPTIDES ON *GIBBERELLA ZEAE* SPORE GERMINATION AND GROWTH

ABSTRACT

The ascomycetous, filamentous fungus, *Gibberella zeae* causes head blight of wheat and other grains. Head blight reduces wheat-kernel weight and limits yield. *Gibberella zeae* infection also results in deoxynivalenol (DON) accumulation within grain. This, and other mycotoxins, significantly limit the marketability of the infected crop.

Head blight is initiated during the spring when wheat develops flowers and *G. zeae* ascospores and macrocondia are present. Head blight management relies heavily on fungicide applications timed to coincide with ascospore dispersal. Although quantitative head-blight resistance is available in commercial wheat varieties it is only partially effective.

To assist the development of enhanced disease resistance, peptides were identified from combinatorial phage-display libraries that inhibit ascospore germination and germling growth. Two peptides, f3-16 and f8-18, were identified that exhibited binding affinity for germinating ascospores and inhibited pathogen development when displayed in phage-display format or as chemically synthesized molecules.

In either form, the inhibitory effect of each peptide was concentration dependent. At 0.2 μM and 2.0 μM concentrations, synthesized peptide f8-18 inhibited germination of macroconidia and ascospores more effectively than did peptide f3-16. Synthesized peptide f8-18 was also tested for inhibition of elongation of both ascospore and macroconidium germ-tubes. At a 0.2 μM concentration, this peptide delayed germ-tube initiation of both spore types and delayed further elongation over a 10-h incubation

period. No spore type produced germ-tubes when incubated in 2.0 μM f8-18. In addition to inhibition of germ-tube elongation, each peptide induced modifications in the germinated morphology of germinating ascospores. At each concentration, germ-tubes emerged more from both apical and intercalary cells of ascospores in comparison to ascospores in control treatments. In addition, the germ-tubes produced from spores incubated in the presence of either peptide had greater diameters than the germ-tubes grown only in a minimal growth medium.

Further confirmation of pathogen inhibition by these peptides in planta is necessary before development of transgenic wheat for further resistance testing.

INTRODUCTION

The filamentous ascomycete, *Gibberella zeae* (Schwien.) Petch (anamorph *Fusarium graminearum* Schwabe), is the most important causal agent of head blight (scab) of wheat and other small grains in North America (9). The fungal pathogen infects and colonizes developing wheat heads, reducing wheat-kernel weight and limiting yield (9). *Gibberella zeae* also produces deoxynivalenol (DON) and other harmful mycotoxins during host colonization that can significantly limit the marketability of a diseased crop (2,9).

Wheat heads are most susceptible to *G. zeae* infection during the anthesis period in spring, when the palea and lemma of wheat florets have opened, anthers have emerged and pollen is dispersed (9,10). *Gibberella zeae* infection is initiated by ascospores that are forcibly discharged from perithecia that mature at this time on plant debris (9,10,23). Ascospores that fall on wheat heads germinate and develop germ-tubes that elongate through the opening between the pelea and lemma to directly penetrate the reproductive tissues without formation of an appressorium (10). Macroconidia are asexual spores of *G. zeae* that can also infect wheat florets. However, macroconidia are generally produced later in growing season and rarely contribute to new floral infections (9,11).

A possible head blight-management strategy would be to deploy inhibitory peptides to reduce ascospore germination and germ-tube development sufficiently to protect wheat plants from infection during anthesis (3,6,7,16). Previous studies have shown that peptides derived from combinatorial phage-display libraries can be selected to effectively inhibit the development of plant pathogens and protect host plants from infection. For example, Bishop-Hurley, et al. (3) selected peptides from combinatorial

libraries with binding affinity for zoospores of the biotrophic oomycete, *Phytophthora capsici.* Several of these peptides were found to induce premature zoospore encystment. When the peptides were expressed in tomato hairy-roots, they induced zoospore encystment at a distance from the root surface and subsequently reduced root infection (6). More recently, Fang, et al (7) selected peptides that bind to germ-tubes of urediniospores produced by *Phakopsora pachyrhizi,* the fungal pathogen that causes Asian soybean rust (7). Several of these peptides were shown to delay infection of soybean leaves when urediniospores and peptides were coinoculated onto soybean leaves.

On the basis of these successes, experiments were conducted to evaluate the potential for identifying inhibitory peptides that interrupt the development of germinating spores of *G. zeae*. The goals of these experiments were i) to identify peptides from combinatorial phage-display libraries with binding affinity for binding to germinating *G. zeae* spores, and ii) to characterize the effects of selected peptides on spore germination and germ-tube growth.

MATERIALS AND METHODS

Fungal isolates and culture conditions. *Gibberella zeae* PH-1 (NRRL 31084) was used in all experiments. To prepare the pathogen for stable, long-term storage, fresh carrot agar (5) was inoculated and incubated in the dark at 24˚C until the fungal mycelium had colonized the medium. The culture was then macerated using a sterile mortar and pestle. One ml of glycerol (35%; v/v) was mixed with the macerated culture using a sterile spatula, and the resulting mycelial suspension was aliquoted into sterile microcentrifuge tubes. The tubes were then flash-frozen by submersion in liquid-phase nitrogen and

immediately placed into a low-temperature freezer (-80 ˚C). For laboratory experiments, a stock culture of *G.zeae* was prepared by inoculating potato dextrose agar (PDA) with a small portion of the stored culture.

Production of macroconidia and ascospores. To produce macroconidia, a small fragment of aerial hyphae was transferred from the margin of a stock culture to Spezieller Nährstoffarmer Agar (SNA), a nutrient-poor medium commonly used for production of macroconidia (14). Inoculated cultures were incubated at room temperature under continuous illumination produced by a combination of fluorescent (cool-white; 40-watt, GE, Fairfield, CT) and near-ultra violet lighting (350 nm; BuyLighting.com, Burnsville, MN). Macroconidia were produced after 10 d of incubation and were harvested by flooding cultures with 3 to 5 ml of minimal medium (MM; 5). Minimal medium was used in all experiments to ensure consistent macroconidium and ascospore germination. After flooding, the agar surface was rubbed with a sterile wire loop, and the macroconidial suspension was passed through one layer of sterile Miracloth (EMD Millipore, Darmstadt, Germany) to remove hyphal fragments.

To produce ascospores, perithecia were produced by modified methods of Klittich and Leslie (14). Briefly, fresh carrot agar was inoculated with mycelium removed from the margin of a stock culture. Inoculated medium was then incubated at room temperature under lighting conditions as described previously. After 3 to 5 d incubation, aerial mycelium was removed from the culture surface, and 500 µl of Tween 20 (2.5% v/v; polyoxyethylene-20-sorbitan) was applied and spread gently with a sterile glass rod. The cultures were incubated for an additional 24 to 48 h under continuous illumination to induce perithecium formation. Mature perithecia were formed after 4 to 7 days additional

incubation. Ascospores were discharged from mature perithecia over a period of 10 to 14 d.

To harvest ascospores of similar age, the lids of Petri dishes that contained mature perithecia were replaced with new lids. After an additional overnight incubation under continuous illumination, the cultures were moved to a laboratory countertop and incubated at room temperature for 20 min. At that time the lids were removed, inverted, and flooded with 2 ml MM to collect adhered ascospores.

Selection of phage-display peptides with affinity for germinating *G. zeae* macroconidia. Peptides with binding affinity for germinated macroconidia were selected from two combinatorial phage-display libraries. One phage-display library, f8 (kindly provided by George P. Smith, University of Missouri, Columbia, MO), consisted of the fd bacteriophage strain modified to express a random 8-amino-acid peptide at the N-terminus of the major coat protein VIII (18,20). In wild-type fd-tet phage, 4000 copies of coat protein VIII make up the majority of the phage's rod-like surface. In a modified fd library, each phage expressed a single peptide variant on each copy of coat protein VIII (18,20). The f8 library contained 1.5×10^9 peptide variants and typically, a phage-display peptide clone concentration of 1.5×10^{14} virions ml^{-1} was used for affinity selections.

The second combinatorial library, Ph.D.-12 (Ph.D.-12, New England BioLabs Inc., Ipswich, MA), consisted of M13 filamentous phage and expressed a 12-amino-acid peptide fused to the N-terminus of the minor coat protein III. Each phage in this library displayed one peptide variant on each of five copies of coat protein III (7). For affinity selections from the Ph.D.-12 library, the number of phage-displayed peptide variants and virion concentration were similar to the f8 library (6,7).

Prior to affinity selection, each library was amplified in *Escherichia coli* (BluKan94 or ER2738 for f8 or Ph.D.-12 libraries, respectively) and precipitated twice with polyethylene glycol (PEG). The resulting phage pellet was resuspended in sterile deionized water to yield a phage concentration of ≈1.5 x 10^{14} virions ml^{-1}.

Germinated macroconidia served as the target population for phage display peptide-affinity selection. Macroconidia began to germinate within four hours of harvest and were considered to have completed germination when germ-tubes were three-fourths the length of a spore. Ten µl of a phage-display library were mixed with 2.0 x 10^5 germinated macroconidia in 1 ml of sterile, deionized water in a round-bottom microcentrifuge tube. The phage-macroconidium mixture was incubated at room temperature, with gentle rocking under ambient lighting for 30 min. After incubation, the mixture was centrifuged to pellet germinated spores. The supernatant containing unbound phage was discarded, and the germinated spore pellet was washed 7 to 10 times in sterile deionized water. After the final wash, bound phage-displayed peptides were eluted from germinated spore surfaces by the addition of 200 µl elution buffer (0.1 N glycine-HCl and 1 g bovine serum albumin L^{-1} at pH 2.2). After 10 min of incubation, the phage suspension was neutralized with 40 µl of 1 M Tris-Cl (pH 9.0). The eluate was amplified in *E. coli* and used for two additional rounds of affinity selection.

Inhibition of spore germination by phage-display peptide clones. Approximately 200 phage-display peptide clones were randomly selected from the third round of affinity selection and assayed for inhibition of macroconidium germination and germ-tube elongation. Thirty µl of a representative phage-peptide clone suspension (1.5 x 10^{11} virion ml^{-1} or 1 nM peptide) was added to 2.0 x 10^5 macroconidia in 1 ml of minimal growth

medium. After 10 min incubation, a 15-µl droplet containing about 2000 spores was placed on a microscope slide fitted with a silicon gasket. A glass cover slip was placed over the gasket to create an incubation chamber. Microscope slides with replicate droplets of the macroconidium-phage mixture were incubated for 12 h in the dark at 24°C. Every two h through the 12-h incubation period, macroconidia were observed in random microscope fields under 100x magnification, and images were captured with a Spot Insight Color digital camera (Diagnostic Instruments, Inc., Sterling Heights, MI) for evaluation of germination and germ-tube elongation. Phage-display peptide clones that induced a notable inhibition of macroconidium germination and germ-tube elongation, relative to macroconidia incubated in MM only, were evaluated in at least two additional trials over the same 12-h period.

Influence of phage-display peptide concentration on spore germination. Two phage-display peptide clones, f3-16 and f8-18 found to be inhibitory in initial evaluations were tested for inhibition of spore germination. As before, virions of f3-16 or f8-18 were mixed with 2.0×10^5 macroconidia to yield final clone concentrations of 1.5×10^{11}, 2.4×10^{11}, or 4.0×10^{11} virions ml^{-1} (1, 1.6, or 2.6 nM peptide, respectively). Control treatments included macroconidia incubated in either MM or equivalent concentrations of wild-type phage. After 10 min incubation, replicate 15-µl droplets of macroconidia were placed on microscope slides as before. Macroconidium germination was assessed at 2-h intervals through 12 h incubation. Percentage germination was based on examination of 50 randomly selected macroconidia or ascospores at each time point.

Ascospore germination was also assessed using the same peptide concentrations and control treatments. Germination experiments for macroconidia and ascospores were performed three times.

Clone f8-18 was also evaluated for inhibition of germ-tube elongation over a range of virion concentrations. As before, virions of f8-18 were mixed with 2.0×10^5 macroconidia to yield final clone concentrations of 1.5×10^{11}, 2.4×10^{11}, or 4.0×10^{11} virions ml^{-1}. Control treatments for evaluations of germination included macronidia incubated in either MM or equivalent concentrations of wild-type phage. After 10 min incubation, replicate 15-µl droplets of macroconidia were placed on microscope slides. Germ-tube growth was measured at 2-h intervals over 10 h incubation. At each time point, germ-tube growth was visualized and quantified by image capture and analysis (Spot imaging software (version 4.0.3), Sterling Heights, MI). Average germ-tube length was determined from 25 randomly selected macroconidia.

Ascospore germ-tube elongation was also assessed using the same peptide concentrations and control treatments. Germ-tube elongation for macroconidia and ascospores were performed three times.

RESULTS

Phage-display peptide selection. Of approximately 200 phage-display peptide clones selected for binding affinity to germinated macroconidia, five were found to inhibit germination and germ-tube elongation in initial screening (Tables 1 and 2). Four of the phage-display peptide clones, f3-9, f3-14, f3-16, and f3-31 were derived from the Ph.D.-12 phage-display library. A fifth clone, f8-18, was recovered from the f8 library.

The region of the phage genome of these clones that encoded the inserted peptides was sequenced. Similarly, the encoding regions of 36 and 30 non-inhibitory clones from the Ph.D.-12 and f8 libraries, respectively, were sequenced (DNA Core Laboratory, University of Missouri, Columbia, MO). Nucleic acid sequences were then translated to amino acid sequence (Sequence Manipulation Suite, Version 2). Sequence analysis revealed that each phage-peptide clone from the Ph.D.-12 library contained a unique inserted peptide. In contrast, about 70% of phage-display peptide clones recovered from the f8-library screening were represented by four peptide sequences (Table 3).

Amino-acid sequences of affinity selected phage display peptides were assessed for similarities by ClustalW (European Bioinformatics Institute). As determined by this analysis, the phage-display peptide clones selected from the Ph.D.-12 library did not exhibit any sequence similarities. In comparison, sequence similarities were found among phage-display peptide clones selected from the f8-library library. Of the four redundant peptide sequences represented by clones from this library, all contained an arginine at the second or third amino acid position, and all but one contained a one to three amino-acid aliphatic region flanked by polar amino acids. Additionally, the C-terminus of each peptide was represented by a polar amino acid. The aspartate located at the N-terminus of each peptide was the consequence of this library's construction (Table 2 and 3).

TABLE 1. Sequences and inhibition activity of phage-display peptides from the Ph.D.-12 library with binding affinity to germinated *Gibberella zeae* macroconidia[a]

Phage-display peptide clone	Amino-acid sequence	Inhibition of germination[b]
f3-1	MNLDTVGRSSYY	-[c]
f3-2	ALTPLTRVYSMS	-
f3-3	SGHAMRTPMLYV	-
f3-4	QSYPASPEYMFQ	-
f3-5	TQEPTIALHVYH	-
f3-6	NMHKMKNLVPVP	-
f3-7	GDWTHLRTLSYY	-
f3-8	GQPSWDDSRVEK	-
f3-9	HNLPLMQPSSDA	+
f3-10	NGHLSRPTWFHP	-
f3-11	ATNLQHNSENRT	-
f3-12	DYSVPASLTSPD	-
f3-13	ALHPLTNRHYAT	-
f3-14	VPHPVIWPTHTT	+
f3-15	TTSTQFTYSLSL	-
f3-16	DPYPVDSQYRFR	+
f3-17	TMPLNIGYSPPI	-
f3-18	LSLPHPVYIQSV	-
f3-19	TPHNAAQEMPYN	-
f3-20	TRSPSFDPPSPL	-
f3-21	AMWAPTKPPLHK	-
f3-22	VMTPFSHQVFHS	-
f3-23	HTSATNSAADPR	-
f3-24	YARNNDLRNTIL	-
f3-25	YTNDSTSGDSSR	-
f3-26	TQSDTMLNYTHS	-
f3-27	ATYPVRHIPFAY	-
f3-28	YSGHSTGNGQNL	-
f3-29	QYPPTATLPNTP	-
f3-30	DSRPAGGTWHQR	-
f3-31	TTAKHPGAVHNP	+
f3-32	NVHPDEGNIWKY	-
f3-33	AATHPPEFTHKN	-
f3-34	AQHYPPPPDRPY	-
f3-35	EVHTFKDLPQGS	-
f3-36	SSDSLHRPSQPL	-

[a] Inhibitory activity was evaluated at a phage-display peptide concentration of 1.5×10^{11} virion ml^{-1}

[b] Germination and germ-tube elongation was evaluated from randomly selected microscope fields in comparison to macroconidia incubated in MM

alone. Evaluations were made intwo-h intervals, through a 12-h of incubation MM (5)

[c] - = No notable inhibition of macroconidium germination or germ-tube elongation; + = notable inhibition of macroconidium germination or germ-tube elongation though three independent evaluations.

TABLE 2. Sequences and inhibition activity of phage-display peptides from the f8 library with binding affinity to germinated *Gibberella zeae* macroconidia[a]

Phage-display peptide clone	Amino-acid sequence	Inhibition of germination[b]
f8-1	DPRTNNVS	-[c]
f8-2	DRSSAPAT	-
f8-3	DRNSAPGT	-
f8-4	DRSSAPAT	-
f8-5	DPRTNSST	-
f8-6	DNRTNSAS	-
f8-7	DRNSAPGT	-
f8-8	DPRAVTHT	-
f8-9	DPRAVTHT	-
f8-10	DRNSAPGT	-
f8-11	DPRAVTHT	-
f8-12	ERNSSQTM	-
f8-13	DRSSAPAT	-
f8-14	DRNSAPGT	-
f8-15	DRGSPPTS	-
f8-16	DRNSAPGT	-
f8-17	DRNTTPGT	-
f8-18	DRSTPSGQ	+
f8-19	DRSSAPAT	-
f8-20	DRNSAPGT	-
f8-21	DNRTNSAS	-
f8-22	DRNSAPGT	-
f8-23	DRSSTATQ	-
f8-24	DRSSAPAT	-
f8-25	DNRTNSAS	-
f8-26	DRNSAPGT	-
f8-27	DRSSAPAT	-
f8-28	DPKSSNSM	-
f8-29	DRNTGTSP	-
f8-30	DRNSAPGT	-

[a] Inhibitory activity was evaluated at a phage-display peptide concentration of 1.5 x 10^{11} virion ml^{-1}

[b] Germination and germ-tube elongation was evaluated from randomly selected microscope fields in comparison to macroconidia incubated in MM alone. Evaluations were made intwo-h intervals, through a 12-h of incubation MM (5)

[c] - = No notable inhibition of macroconidium germination or germ-tube elongation; + = notable inhibition of macroconidium germination or germ-tube elongation though three independent evaluations.

TABLE 3. Sequence redundancy of phage-display peptide clones recovered from the f8 library after affinity selection against germinated macroconidia of *Gibberella zeae* [a]

Amino-acid sequence	Number of clones recovered
DRNSAPGT	9
DRSSAPAT	6
DPRAVTHT	3
DNRTNSAS	3

[a] Phage-display peptide clones recovered from third-round affinity-selection eluate.

Inhibition of macroconidium germination by phage-display peptide clones f3-16 and f8-18. Phage-display peptide clones f3-16 and f8-18 inhibited both spore germination and germ-tube elongation. When incubated in MM, macroconidium germination was first detected after 4 h (Figs 1A and 1B). Germination increased rapidly from that point onward and reached a maximum of 98% by 12 h. After about 7 h incubation, 50% of the macroconidia had germinated. Germination of macroconidia incubated with wild-type phage was similar to germination in MM in all experiments (data not shown).

In contrast to control treatments, germination of macroconidia incubated with phage-display peptide f3-16 at concentrations of 1.3×10^{11} or 2.7×10^{11} virions ml^{-1} was first observed after 6 h (Fig 1A). Germination at these virion concentrations increased rapidly to a maximum of 94% after 12 h. However, the time required for 50% germination was delayed and occurred after about 8 h. At the highest concentration of 4.0×10^{11} virions ml^{-1}, macroconidium germination increased more slowly, reaching 50% after 11 h and a maximum of 90% germination after 12 h.

Germination of macroconidia incubated with peptide f8-18 was similar at all virion concentrations. At each virion concentration, germination was first observed after 6 h incubation. Between 6 and 10 h, increases in macroconidium germination were similar to those of macroconidia incubated in MM. After 10 h, an average of 82% of the macroconidia incubated with f8-18 had germinated and no further germination was observed.

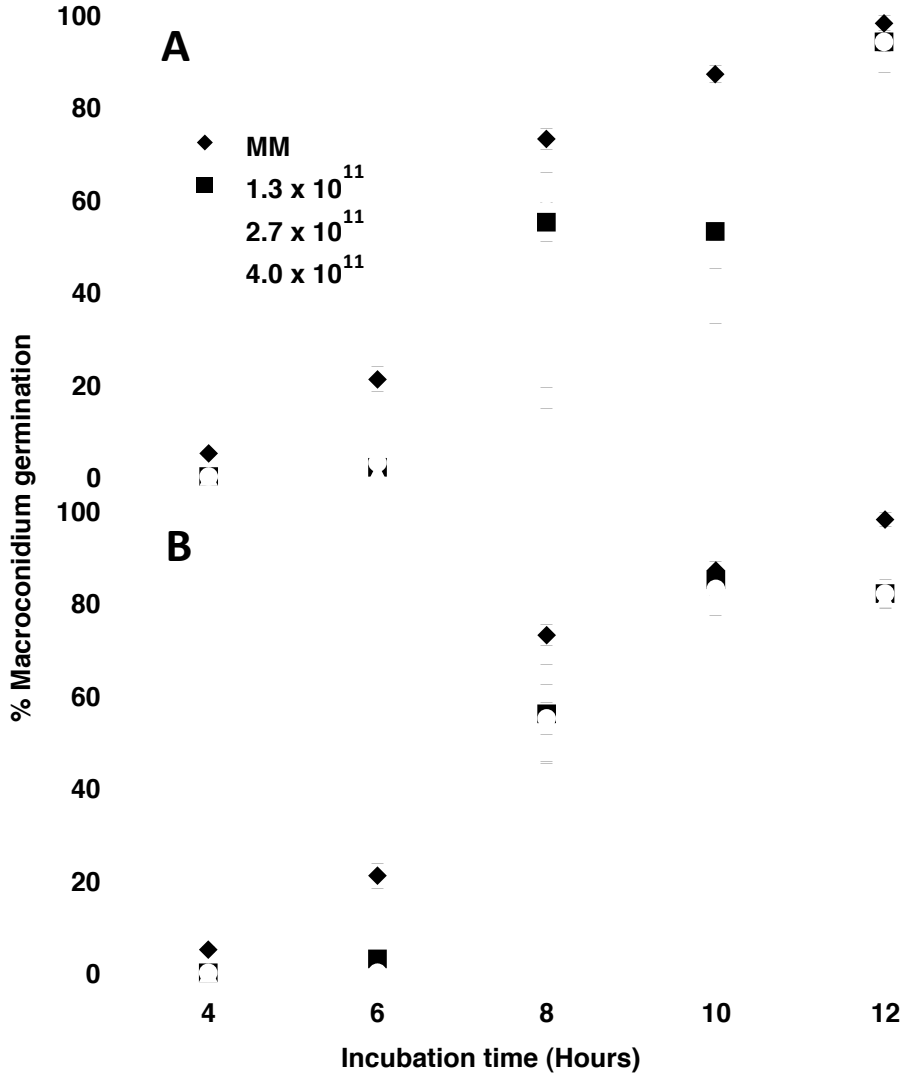

Fig. 1. Germination of *Gibberella zeae* macroconidia in relation to concentration (virions ml^{-1}) of phage-display peptides f3-16 **A**, and f8-18 **B,** or in minimal medium (5). Bars indicate standard error of the mean (n=4).

Inhibition of macroconidium and ascospore germination by synthesized peptides f3-16 and f8-18. Peptides f3-16 and f8-18 were also evaluated in a non-phage-display format as synthesized molecules. For these experiments, each peptide was commercially synthesized (CelTek Peptides, Nashville, TN), prepared for use by dissolving in dimethylformamide, followed by dilution with MM to 0.2 and 2.0 μM concentrations for inhibition assessment.

In MM, macroconidium germination averaged 4.5% after 6 h of incubation. After 12 h, germination averaged 97% (Fig 2A and B).

In contrast to germination in MM, synthesized peptide f3-16 at a concentration of 2.0 μM completely inhibited germination of macrocondia through 12 h incubation (Fig 2A). However, germination of macroconidia incubated with 0.2 μM f3-16 averaged 1 % after 6 h incubation, and after 12 h, macroconidium germination averaged 83% (Fig. 2A)

At 2.0 μM concentration, synthesized peptide f8-18 also completely inhibited macroconidium germination through 12 h incubation. In comparison, germination of macroconidia in 0.2 μM f8-18 was similar to germination in MM and averaged about 1 and 98% after 6 and 12 h incubation, respectively (Fig. 2B).

Ascospores incubated in MM germinated much faster than macroconidia. After 6-h incubation, an average of 100% had germinated (Fig. 3A and B).

At 2.0 μM concentration, peptides f3-16 and f8-18 also inhibited ascospore germination. At this concentration, no germination of ascospores was observed after 6 h incubation. By 12 h, 8% or 0% of ascospores had germinated when incubated with peptide f3-16 or f8-18, respectively (Fig. 3A and B). Germination of ascospores incubated in 0.2 μM f3-16 did not differ significantly from germination in MM.

At a concentration of 0.2 µM f8-18, ascospores did not germinate. However, by 12 h, ascospore germination had reached an average of 89% (Fig. 3B).

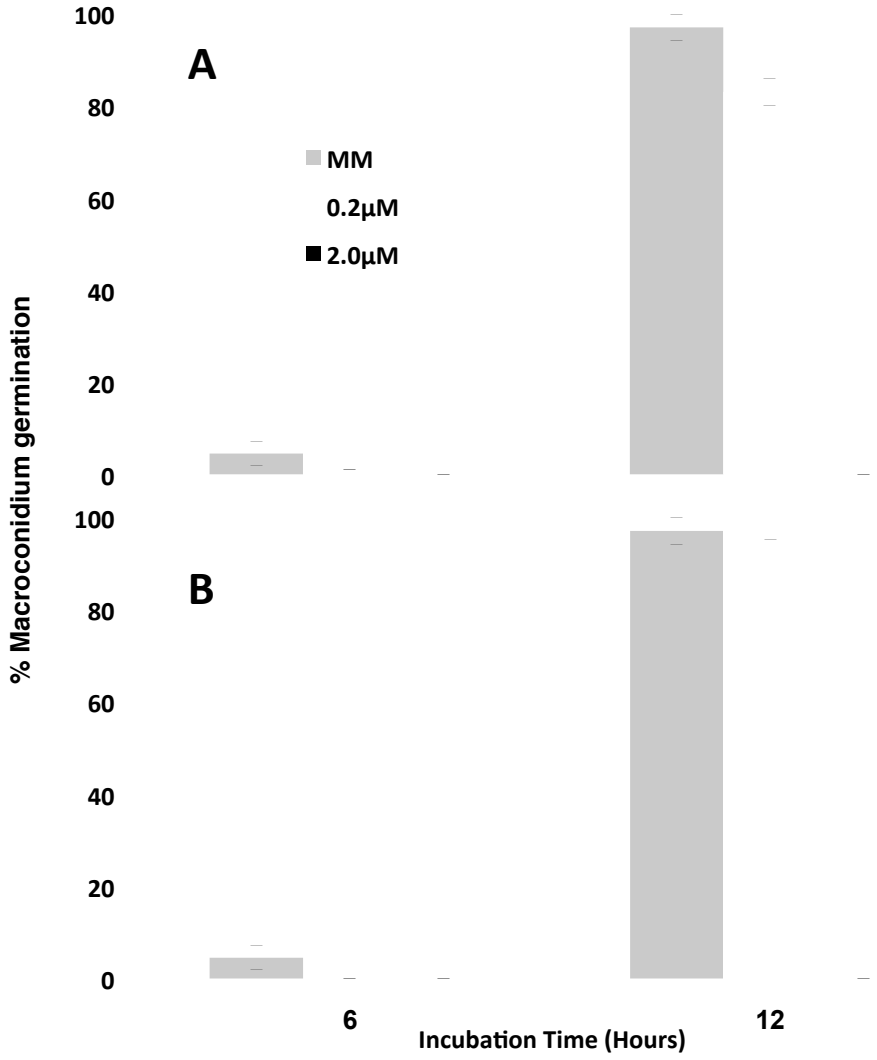

Fig 2. Germination of *Gibberella zeae* macroconidia in relation to concentration of synthesized peptides f3-16 **A**, and f8-18 **B,** or in minimal medium (5). Bars indicate standard error of the mean (n=4).

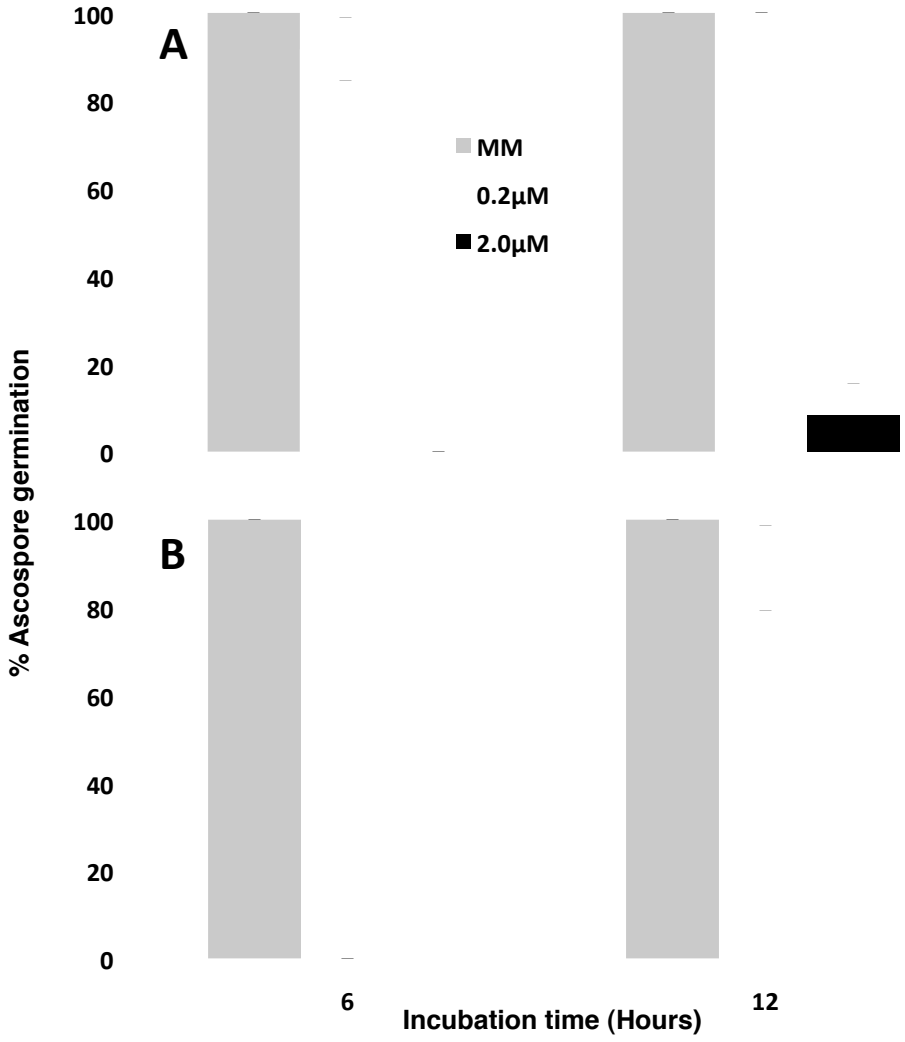

Fig 3. Germination of *Gibberella zeae* ascospores in relation to concentration of synthesized peptides f3-16 **A**, and f8-18 **B,** or in minimal medium (5). Bars indicate standard error of the mean (n=4).

Inhibition of macroconidium and ascospore germ-tube elongation by synthesized peptide f8-18. Macroconidium germ-tube elongation was inhibited by synthesized peptide f8-18. When incubated in MM for 4 h, macroconidia germinated and produced germ-tubes that averaged 9.4 μm in length (Fig. 4A). Germ-tubes continued to elongate steadily over the next 6 h and attained a maximum average length of 120.4 μm by 10 h.

In contrast, when incubated in 0.2 μM f8-18, macroconidium germ-tubes elongated more slowly and averaged only 2.8 μm by 6 h incubation. Then, germ-tubes continued to slowly elongate from that time point and reached a maximum average length of 37.4 μm by 10 h incubation (Fig. 4A). Even greater inhibition of germ-tube elongation was observed when macroconidia were incubated in 2.0 μM f8-18. Under these conditions germ-tube length could not be accurately measured due to limitations in the Spot analytical software. By visual observation however, very few of these spores would have been considered germinated under the pre-described criteria.

Peptide f8-18 also inhibited ascospore germ-tube elongation. In these experiments, ascospores incubated in MM developed germ-tubes that averaged 31.5 μm in length after 4 h incubation (Fig. 4B). From that time onward, germ-tubes elongated progressively, reaching a maximum length of 127 μm after 8 h incubation. No additional germ-tube elongation occurred through 10 h incubation.

Delays in germ-tube elongation occurred when ascospores were incubated in either 0.2 μM or 2.0 μM f8-18. After 4 h of incubation at either peptide concentration, no germ-tubes were produced (Fig. 4B). By 6 h incubation in 0.2 μM f8-18, ascospore germ-tubes averaged 11 μm in length. Further elongation occurred slowly from this point onward, and after 10 h incubation, average germ-tube length reached a maximum of 76.5

μm. When incubated in 2.0 μM f8-18, ascospores did not germinate sufficiently to allow measurement of germ-tubes.

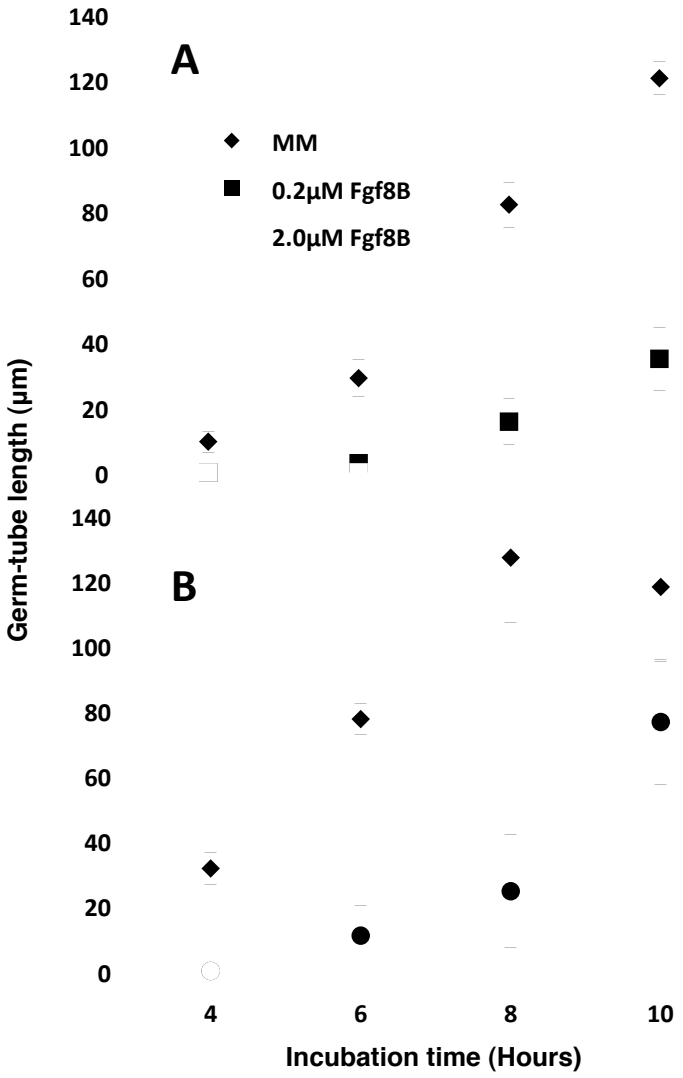

Fig 4. Germ-tube elongation of *Gibberella zeae* macroconidia **A**, and ascospores **B**, in relation to concentration of peptide f8-18 or in minimal medium (5). Bars indicate standard error of the mean (n=3).

.

Influence of synthesized f3-16 and f8-18 on germinated ascospore morphologies. Ascospores incubated with peptide f3-16 or f8-18 exhibited germ-tube morphologies that differed from ascospores incubated in MM (Table 4 and 5 ; Fig. 5). Ascospores incubated for 10 h in MM produced a single germ-tube from one apical cell about 77% of the time, while the remaining ascospores produced one germ-tube from each apical cell (Fig. 5A). Germ-tubes never developed from an intercalary cell. Germ-tubes were generally uniform in diameter from germ-tube base to the point of emergence. After 10 h incubation, 43% of ascospore germ-tubes had branched to produce 1 to 3 lateral hyphae. The remaining ascospores produced unbranched germ-tubes.

When incubated for 10 h in 0.2 μM f3-16 or f8-18, 50% of ascospores produced a germ-tube from one apical cell and the remaining spores produced germ-tubes from the two apical cells (Fig. 5B). In addition, about 17% of these ascospores incubated with either peptide produced a germ-tube from one or more intercalary cells. The diameters of ascospore germ-tubes incubated with either peptide were noticeably greater than the diameter of those ascospores germinated in MM. After 10 h incubation, ascospores produced only unbranched germ-tubes.

When ascospores were incubated in 2.0 μM f3-16 or f8-18, a germ-tube was often initiated from a single apical cell but did not elongate. These germ-tubes commonly consisted of only a single cell, 4 μm or less in length, and the cell was often swollen to a diameter nearly equivalent to the ascospore diameter.

TABLE 4. Germ-tube morphological attributes of germinated *Gibberella zeae* macroconidia[a]

Number of germ-tubes (%)		Branch points per germ-tube (%)			
1	**2**	**0**	**1**	**2**	**3**
76.7 (± 8.8)[b]	23.3 (± 8.8)	23.3 (± 8.8)	26.7 (± 6.6)	6.7 (± 6.6)	10 (± 0)

[a] Data was collected from images captured during germination and germ-tube elongation experiments

[b] Variance determined by standard error of the means (n=3).

TABLE 5. Germ-tube morphological attributes of germinated *Gibberella zeae* macroconidia incubated in 0.2 µM f8-18[a]

Germ-tubes per conidia (%)		Swollen germ-tubes (%)	Germ-tube emergence from intercalary ascospore cell (%)
1	2		
50 (± 11.6)[b]	50 (± 11.6)	90 (± 2.3)	16.7 (± 3.3)

[a] Data was collected from images captured during germination and germ-tube elongation experiments

[b] Variance determined by standard error of the means (n=3).

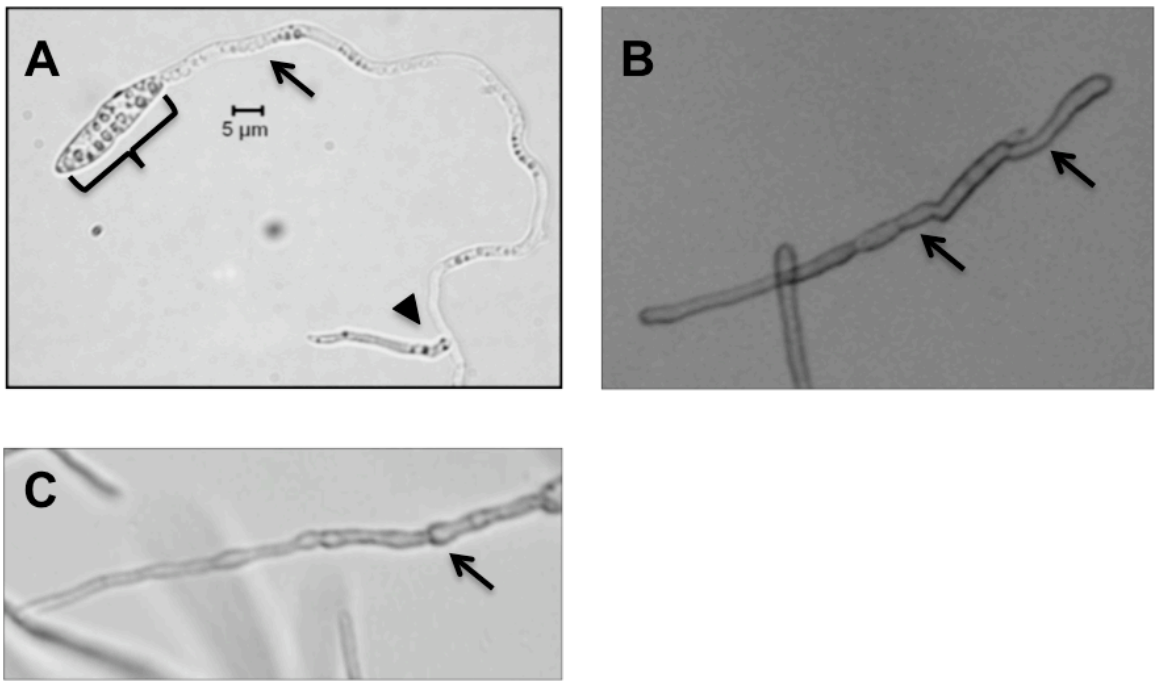

Fig. 5. *Gibberella zeae* gross morphology after 10 hour incubation with peptide f3-16. Ascospores incubated 10 h in minimal medium (5) **A**, or 0.2 µM f3-16 **B** and **C**. Normally germinating ascospore (bracket), germ-tube (arrow) of uniform diameter, emerged from apical germ-tube cell, and lateral branch point (arrow head) **A**. Germ-tubes (arrows) of variable diameter emerging from two apical ascospore cells treated with 0.2 µM f3-16, **B**. Germinated ascospore treated with 0.2 µM f3-16, unevenly swollen germ-tube (arrow) **C**.

DISCUSSION

Two peptides were selected from combinatorial phage-display peptide libraries that inhibited germination and early growth of both macroconidia and ascospores of *G. zeae*. The peptides f3-16 and f8-18 were 8 and 12 amino acids in length, respectively, and they did not exhibit any similarities in primary structure. However, these peptides were similar in their inhibition effects. For example, each of these peptides, when chemically synthesized, inhibited germination of macroconidia and ascospores in a concentration-dependent manner. At 2.0 μM concentration, each of these peptides completely inhibited germination over a 12-hr incubation period. Peptide f8-18 was also found to delay germ-tube elongation of macroconidia and ascospores at 0.2 μM concentration.

The identification of unrelated peptides with similar inhibition is not surprising because it is possible that each peptide interacted with different factors on the surfaces or within the cells of spores and germ-tubes that contribute to reduced germination and growth. Montgomery-Smith and Schmidt (17) and Bishop-Hurley et al. (3) described this possibility and suggested that whole cells of any organism would display a diverse population of molecular targets for peptide interactions.

This is the first demonstration of selection of phage-display combinatorially selected peptides that inhibit germination and early growth of fungi within the Ascomycota. These studies extend previous reports of inhibitory peptide selection that disrupt development of *Phakopsora pachyrhizi*, a member of the Basidiomycota (7), and *Phytophthora capsici* (3,6), an oomycetous organism located in Kingdom Stramenopila. As in the development of inhibitory peptides directed against *P. pachyrhizi* and *P. capcisi*, the selection of inhibitory peptides directed at *G. zeae* required minimal time and

effort. After completion of a peptide-screening protocol, approximately 6 months was required to proceed from initial affinity selection of peptides to characterization of their inhibitory potential.

In initial affinity selection, only five clones were identified from combinatorial libraries that inhibited germination of *G. zeae* macroconidia. This was fewer than the number of peptides identified as inhibitory to urediniospore germination in *P. pachyrhizi*. The difference in richness of the candidate peptide pools may be the result of the methods used to assess inhibition. In the case of *P. pachyrhizi*, peptide inhibition was measured by significant reduction in uriediniospore germ-tube elongation in comparison to germ-tube growth in water. In the current work, inhibition was measured based on a defined percentage of spore germination rather than relative germ-tube length to a control. It would be expected that fewer clones would be selected based on this more stringent criterion of inhibition.

In addition to reductions in germination and germ-tube elongation, peptides f3-16 and f8-18 induced aberrations in the morphology of germinating ascospores. In particular, each peptide induced modified germ-tube emergence and branching patterns. In addition germ-tubes of variable diameter were formed when incubated with f3-16 or f8-18. These morphological aberrations could be the result of abnormal apical cell elongation caused by a disruption in germ-tube polarity. Morphological alterations, similar to those noted in this study have been observed in similar studies to identify fungal inhibitory peptides (16). However, at higher concentrations of peptide, hyphal collapse, indicating cell death, was observed (16). This work used relatively low concentrations of peptide. Typical, effective concentrations of antimicrobial peptides

range from 1 to 20 μM (16). Perhaps higher peptide concentration would induce similar effects in *G. zeae.*

In addition to combinatorially selected peptides, pheromone mating peptides derived from *G. zeae* have been reported to inhibit germination of both macroconidia and ascospores. Lee and Leslie (15) reported that these peptides, and their derivatives based on specific amino acid substitutions, effectively inhibited germination of both ascospores and macroconidia, at peptide concentrations within the same range as those discussed in this study. The mating pheromone peptides were 10 to 11 amino acids in length, but their primary structures bore no resemblance to peptides f3-16 or f8-18. The assemblage of diverse peptides that produce similar inhibition phenotypes in *G. zeae* offers a unique opportunity to investigate the range of mechanistic pathways by which fungal hyphae perceive and respond to inhibitory molecules in their surrounding environment.

Additional work must be carried out, however, to determine whether these peptides are toxic to either wheat or animals. Additionally, more studies must be carried out to determine the mode of action of f3-16 and f8-18, also to determine their potential toxicity.

The inhibition exhibited by peptides f3-16 and f8-18 in these in vitro studies provides an early indication of potential for effective inhibition of *G. zeae* infection in planta. When deployed and expressed in transgenic wheat, hyphae of *G. zeae* colonizing host tissues would be exposed constantly to one or more of these peptides, and the inhibition observed in these short-term experiments would extend through much longer time periods. Thus, when expressed in an already partially resistant wheat plant,

inhibitory peptides f3-16 and f8-18 may enhance head blight protection in wheat production fields.

LITERATURE CITED

1. Beyer, M. and Verreet, J-A. 2005. Germination of *Gibberella zeae* ascospores as affected by age of spores after discharge and environmental factors. Eur. J. Plant Pathol. 111:381-389.
2. Beyer, M., Verreet, J-A., and Ragab, W. S. M. 2005. Effect of relative humidity on germination of ascospores and macroconidia of *Gibberella zeae* and deoxynivalenol production. Int. J. Food. Microbiol. 98:233-240.
3. Bishop-Hurley, S. L., Mounter, S. A., Laskey, J., Morris, R. O., Elder, J, Roop, P., Rouse, C., Schmidt, F. J., and English, J. T. 2002. Phage-displayed peptides as developmental agonists for *Phytophthora capsici* zoospores. App. Environ. Mircobiol. 68:3315-3320.
4. Bishop-Hurley, S. L., Schmidt, F. J., Erwin, A. L., Smith, A. L. 2005. Peptides selected for binding to a virulent strain of *Haemophilus influenzae* by phage display are bactericidal. Antimicrob. Agents Chemother. 49:2972-2978.
5. Correll, J. C., Klittich, C. J. R., and Leslie, J. F. 1987. Nitrate nonutilizing mutants for *Fusarium oxysporum* and their use in vegetative compatibility tests. Phytopathology. 77:1640-1646.
6. Fang, Z. D., Laskey, J. G., Huang, S., Bilyeu, K. D., Morris, R. O., Schmidt, F. J., and English, J. T. 2006. Combinatorially selected defense peptides protect plant roots from pathogen infection. Proc. Natl. Acad. Sci. USA 103:18444-18449.

7. Fang, Z. D., Marois, J. J., Stacey, G., Schoelz, J. E., English, J. T., and Schmidt, F. J. 2010. Combinatorially selected peptides for protection of soybean against *Phakopsora pachyrhizi*. Phytopathology 100:1111-1117.
8. Fernando, W. G. D., Miller, J. D., Seaman, W. L., Seifert, K., and Paulitz, T. C. 2000. Daily and seasonal dynamics of airborne spores of *Fusarium graminearum* and other *Fusarium* species sampled over wheat plots. Can. J. Bot. 78:497-505.
9. Goswami, R. S., and Kistler, H. C. 2004. Pathogen profile: Heading for disaster: *Fusarium graminearum* on cereal crops. Mol. Plant Pathol. 5:515-525.
10. Guenther, J. C. and Trail, F. 2005. The development and differentiation of *Gibberella zeae* (anamorph: *Fusarium graminearum*) during colonization of wheat. Mycologia 97:229-237.
11. Harris, S. D. 2005. Morphogenesis in germinating *Fusarium graminearum* macroconidia. Mycologia 97:880-887.
12. Harris, S. D., Hofmann, A. F., Tedford, H. W., and Lee, M. P. 1999. Identification and characterization of genes required for hyphal morphogenesis in the filamentous fungus *Aspergillus nidulans.* Genetics. 151:1015-1025.
13. Hill, D. F., Pertersen, G. B. 1982. Nucleotide sequence of bacteriophage f1 DNA. J. Virol. 44:32-46.
14. Klittich, C. J. R. and Leslie, J. F. 1988. Nitrate reduction mutants of *Fusarium moniliforme* (*Gibberella fujikuroi*). Genetics 118:417-423.
15. Lee, J. K. Alignment between genetic and physical map, and pheromone functions in *Gibberella zeae.* Ph. D. Dissertation. Kansas State University. http://hdl.handle.net/2097/562

16. Marcos, J. F., Muñuz, A., Pérez-Payá, E., Misra, S., and López-García, B. 2008. Identification and rational design of novel antimicrobial peptides for plant protection. Annu. Rev. Phytopathol. 46:273-301.
17. Montgomery-Smith, S. J and Schmidt, F. J. Statistical methods for estimating complexity from competition experiments between two populations. J. Thero. Biol. 264:1043-1046.
18. Petrenko, V. A., Smith, G. P., Gong, X. and Quinn, T. 1996. A library of organic landscapes on filamentous phage. Protein Eng. 9:797-801.
19. Seong, K-Y., Zhao, X., Xu, J-R., Güldener, U., and Kistler, H. C. 2008. Conidial germinaiton in the filamentous fungus *Fusarium graminearum.* Fungal Genet. Biol. 45:389-399.
20. Smith, G. P. and Petrenko, V. A. 1997. Phage Display. Chem. Rev. 97:391-410.
21. Stothard P. 2000. The sequence manipulation suite: JavaScript programs for analyzing and formatting protein and DNA sequences. Biotechniques 28:1102-1104.
22. Sudbery, P. 2011. Review: Fluorescent proteins illuminate the structure and function of the hyphal tip apparatus. Fungal Genet. Biol. 48:849-857.
23. Trail, F., Common, R. 2000. Perithecial development by *Gibberella zeae:* a light microscopy study. Mycologia 92:130–138.
24. Xu, X-M., Monger, W., Ritieni, A., and Nicholson, P. 2007. Effect of temperature and duration of wetness during initial infection periods on disease development, fungal biomass and mycotoxin concentrations on wheat inoculated with single, or combinations of, *Fusarium* species. Plant Pathol. 56:943-956.

25. Yu, J. and Smith, G. P. 1996. Affinity maturation of phage-displayed peptide ligands. Methods Enzymol. 267:3-27.

CHAPTER THREE

RELATIONSHIP OF INHIBITORY PEPTIDES TO CYTOLOGICAL ATTRIBUTES OF POLARIZED GROWTH OF GERMINATING *GIBBERELLA ZEAE* ASCOSPORES

ABSTRACT

The ascomycete *Gibberella zeae* causes head blight of wheat and other grains. Head blight reduces wheat-kernel weight and limits yield. *Gibberella zeae* infection also results in mycotoxin accumulation within harvested grain, which significantly limits the marketability of the crop.

To enhance wheat resistance to head blight, peptides were identified from combinatorial phage-display libraries that inhibit ascospore germination and germ-tube growth. Two peptides, f3-16 and f8-18, were identified pathogen-affinity selected collections that inhibit germ-tube growth and induce aberrant germ-tube morphology.

Experiments were conducted to evaluate whether inhibitory peptide f3-16 affect constituents of the germ-tube apical cell that are important for polarized elongation, including endocytic system components, sterol-rich plasma membrane domains (SRD), and patterns of cell wall deposition.

When incubated in a minimal growth medium, *G. zeae* ascospore germ-tubes were stained to visualize components of the endocytic system, plasma membrane, endocytic vesicles, endosomes, and Spiztenkörper. These components were stained in the same temporal sequence that was observed in similar experiments with *Aspergillus nidulans* and other filamentous fungal species. Staining of SRDs and cell-wall chitin was concentrated at polar-tips of apical germ-tube cells of *G. zeae* and at points of septations, which also agrees with previous observations in *A. nidulans* and other filamentous fungi.

When ascospores were incubated with the inhibitory peptide f3-16, and resulting germ-tubes were stained, the timing of stain uptake by plasma membrane, endocytic vesicles, and endosomes did not differ from that of normally germinating spores. However, endosomes densely accumulated within the germ-tube cytoplasm, and vacuole formation appeared to be inhibited. The distributions of SRDs and chitin deposition were also altered in ascospore germ-tubes incubated with peptide f3-16. These cellular components were observed in only patchy distribution throughout remaining subapical regions of the germ-tube.

This study provides the first description of cytological changes in germinating ascospores induced by a combinatorially selected inhibitory peptide. The characterized cytological phenotypes provide the ground work for mechanistic studies of growth inhibition and morphological modifications caused by inhibitory peptides.

INTRODUCTION

The filamentous ascomycete, *Gibberella zeae* (Schwein.) Petch (anamorph *Fusarium graminearum* Schwabe) is the most important causal agent of head blight (scab) of wheat and other small grains in North America (20). The fungal pathogen infects and colonizes developing wheat heads, reducing wheat-kernel weight and limiting yield (20). *Gibberella zeae* also produces deoxynivalenol (DON) and other harmful mycotoxins during host colonization that can significantly limit the marketability of an affected crop (20).

Wheat heads are most susceptible to *G. zeae* infection during the anthesis period in spring. At that time the palea and lemma of wheat florets open, anthers emerge and pollen disperses (20). *Gibberella zeae* infection is initiated by ascospores that are forcibly discharged from perithecia that mature at this time on plant debris (20,21,45). Ascospores that fall on wheat heads germinate and develop germ-tubes that elongate through the opening between the palea and lemma to directly penetrate the reproductive tissues, without formation of an appressorium (20,21). Macroconidia are asexual spores of *G. zeae* that can also infect wheat florets. However, macroconidia are generally produced later in the growing season and rarely contribute to new floral infections (20).

A possible head-blight management strategy would be to deploy inhibitory peptides to sufficiently reduce ascospore germination and germ-tube development to protect plants from *G. zeae* infection during anthesis (4,15,16,30). Previous studies have shown that peptides derived from combinatorial phage-display libraries can be selected to effectively inhibit the development of fungal and oomycetous plant pathogens. For example, Bishop-Hurley et al (4) selected peptides from combinatorial libraries with

binding affinity for zoospores of the biotrophic oomycete, *Phytophthora capsici.* Several of these peptides were found to induce premature zoospore encystment. When the peptides were expressed in tomato hairy-roots, they induced zoospore encystment at a distance from the root surface and subsequently reduced root infection (16). More recently, Fang et al (16) selected peptides that bind to germinating urediniospores produced by *Phakopsora pachyrhizi,* the fungal pathogen that causes Asian soybean rust (16). Several of these peptides were shown to delay infection of soybean leaves when urediniospores and peptides were coinoculated onto soybean leaves.

Peptides derived from combinatorial phage-display libraries have recently been identified that inhibit germination and germ-tube elongation of *G. zeae* ascospores and macroconidia. The peptides also induced aberrant germination morphologies such as variable emergence of thickened germ-tubes with reduced length. These developmental abnormalities caused by inhibitory peptides may be related to disruption of polarized growth in *G. zeae* (22,24,30).

Studies of hyphal morphogenesis and polar growth in *Saccharomyces cervisiae* and also in filamentous ascomycetes, such as *Aspergillus nidulans* and *Neurosopora crassa*, have revealed that fungal growth requires the transport of Golgi-body derived membrane-bound vesicles to the germ-tube apical cell tip (9,23,33,34,43,46). Vesicles are trafficked along microtubule filaments to an apical vesicle-organization complex, the Spitzenkörper, and from there they are sorted within an actin-mediated complex for delivery and localization to the elongating polar tip of the germ-tube apical cell where the vesicles are exocytosed. Contents of apically delivered vesicles include both transmembrane and soluble molecules that serve biological roles in cell functioning such

as construction, signaling, and nutrient acquisition (9,12,37,40,47). In addition, exocytic fusion of vesicles to the polar cell apex increases the surface area of the membrane resulting in cell elongation (9,12,33,37,40,47).

As the plasma membrane surface area increases at the cell apex, plasma membrane is also internalized subapically by endocytosis (1,33,43,46). During endocytosis, plasma membrane with associated proteins and other molecules derived from the cell and from the external environment are enveloped in plasma membrane to form structures known as endocytic vesicles. These disassociate from the plasma membrane to form small, spherical early endosomes, which are transported along microtubule filaments to the Spitzenkörper, sorted, and trafficked back to be incorporated into vacuoles where their contents are stored or degraded (1,33,43,46).

The spatial and temporal patterns of the endocytic process have been studied in filamentous fungi by visualization with the fluorescent stain FM4-64 (1,33,43,46). This stain functions by incorporation into inner-leaflets of lipid membranes that comprise structural components of the endocytic system, including the cell plasma membrane, septum-associated membranes, endocytic vesicles, early endosomes, vacuoles, and exocytic vesicles (1,33,43,46). For example, by FM4-64 staining, Atkinson et al. (3) characterized specific steps in the endocytic processes during conidium germination of the fungal rice pathogen, *Magnaporthe grisea* (3). The specificity of FM4-64 staining of endocytic system components in filamentous fungi was confirmed by comparison with the other common endocytic-marker stains, Lucifer Yellow carbohydrazide and FITC-dextran. These stains function similarly to FM4-64 in that they are plasma-membrane impermeable and are endocytosed along with regions of plasma membrane (3). Later,

Peñalva (33) characterized the endocytic system in germinated conidia of *A. nidulans* and validated specificity of FM4-64 vacuolar lumen staining with CDCFDA. These studies, and others have confirmed that FM4-64 is able to accurately visualize membrane components of fungal endocytic systems.

Proteins integrated into the plasma membrane at the polar axis of the apical germ-tube cell via vesicle fusion are not sorted to produce a spatially homogeneous array, but instead aggregate within specific membrane regions (14,23,24,36). The aggregation of membrane-associated proteins is partially affected by the distribution of sterol rich domains (SRDs) within the plasma membrane (23,24,36). In fungi, the most abundant plasma membrane sterol is ergosterol (23,35). In addition to influences on protein aggregation, SRDs have been shown to affect polarized hyphal growth by presumably enabling anchoring of cytoskeletal filaments involved in vesicle trafficking (35,45). Rittenour et al. (35) also established that SRDs are involved with successful host infection by the pathogen by maintaining polarized growth of infective hyphae.

Sterol rich domains within the hyphal plasma membrane are typically localized to polar tip of the apical cell, but SRDs are also observed at points of septum formation (35). The distribution of SRDs in the hyphal plasma membrane has been visualized by staining with filipin, a naturally fluorescent polyene antibiotic that binds strongly with sterols (23,24,35,36).

The cell wall is synthesized at the polar tip of the apical hyphal cell, and in conjunction with the formation of hyphal septa (10,12,22,29). When initially synthesized, the cell wall is initially thin, elastic, and consists primarily of chitin chains, composed of β1,4-linked *N*-acetylglucosamine subunits that form strong hydrogen bonds among

adjacent chains to develop fibrils. Polymerization of *N*-acetylglucosamine subunits to form homopolymer chains is mediated by chitin synthase (10,12). When chitin synthase is incorporated in the membrane of the germ-tube apex or septation points via specialized vesicles, termed chitosomes, enzyme activity is highly regulated (10,12). Further modifications of chitin fibrils, and other cell-wall polysaccharides such as β-glucans form a thicker, more complex subapical cell wall (10,12). Glycoprotein components, anchored to the plasma membrane, are also intercalated within the extracellular matrix (10,12). The increasing thickness and subsequent rigidity of subapical germ-tube cells provides structural support and protection from environmental factors (10,12). The cell wall is the initial region of physical contact between a fungal pathogen and a host plant; as such it is an important factor for successful host infection (10,12).

To study the pattern of chitin deposition within *G. zeae* germ-tube cell walls, the lectin, wheat-germ agglutinin (WGA) was used. WGA strongly binds with chitin chains in a predominately N-linked manner (19). Subapically, germ-tube cell walls become thicker and more chemically complex in subapical regions (19). Although chitin may be present, chitin-WGA binding is inhibited because fibrils are masked or modified (19). This attribute allows for the characterization of cell-wall attributes in living filamentous fungi.

The goal of the present study was to evaluate whether inhibitory peptides affect structural components of the germ-tube apical cell that are important for polarized hyphal elongation. Specific objectives were to assess the influence of an inhibitory peptide on i) structural components of the endocytic system, ii) distribution of SRDs, and iii) patterns of cell wall deposition.

MATERIALS AND METHODS

Fungal isolates and culture conditions. *Gibberella zeae* PH-1 (NRRL 31084) was used throughout the study. To prepare the fungus for stable, long-term storage, fresh carrot agar (26) was inoculated and incubated in the dark at 24˚C until the fungal mycelium had colonized the medium. The culture was then macerated using a sterile mortar and pestle. One ml of glycerol (35%; v/v) was mixed with the macerated culture using a sterile spatula, and the resulting mycelial suspension was aliquoted into sterile microcentrifuge tubes. The tubes were then flash-frozen by submersion in liquid-phase nitrogen and immediately placed into a low-temperature freezer (-80 ˚C). For laboratory experiments, a stock culture of *G.zeae* was prepared by inoculating potato dextrose agar (PDA) with a small portion of the stored culture.

Production of ascospores. To produce ascospores, perithecia were produced by modified methods of Klittich and Leslie (26). Briefly, fresh carrot agar was inoculated with mycelium removed from the margin of a stock culture. Inoculated medium was then incubated at room temperature under lighting conditions as described previously. After 3 to 5 d incubation, aerial mycelium was removed from the culture surface, and 500 µl of Tween 20 (2.5% v/v; polyoxyethylene-20-sorbitan) was applied and spread gently with a sterile glass rod. The cultures were incubated for an additional 24 to 48 h under continuous illumination to induce perithecium formation. Mature perithecia were formed after 4 to 7 days additional incubation. Ascospores were discharged from mature perithecia over a period of 10 to 14 d.

To harvest ascospores of similar age, the lids of Petri dishes that contained mature perithecia were replaced with new lids. After an additional overnight incubation under

continuous illumination, the cultures were moved to a laboratory countertop and incubated at room temperature for 20 min. At that time the lids were removed, inverted, and flooded with 2 ml MM to collect adhered ascospores.

Influence of inhibitory peptide f3-16 on structural components of the endocytic system. Peptides f3-16 was synthesized by CelTek Peptides (Nashville, TN). The peptides was received in lyophilized form and dissolved in 2% dimethylformamide, and diluted to a 100 µM concentration. This f3-16 stock solution was stored at -20˚C until used.

Ascospores of *G. zeae,* collected from Petri dish lids, were suspended in 700 µl of MM containing 0.2 µM inhibitory peptide f3-16 and then dispensed into a glass-bottomed culture dish (WillCo Dish, Amsterdam, The Netherlands). The culture was incubated in the dark for 18 h at 24˚C to allow ascospores to germinate and adhere to the bottom of the culture dish. The dish was then washed 3 times with MM to remove non-adhered spores.

After the final wash, adhered germinated ascospores were stained with FM4-64 (FM4-64; Molecular Probes, Invitrogen Corporation, Carlsbad, California) to visualize structural components of the endocytic system. One ml of ice-cold Hank's balanced salt solution (HBSS) without magnesium and containing 10 µM FM4-64 was applied to the adhered germinated ascospores and incubated on ice for 2 min. At that time, excess stain was removed and a cover slip was placed over the germinated ascospores.

Stained germinated ascospores were viewed by laser-scanning confocal microscopy (Zeiss 5-Live or 510-META, Carl Zeiss, Oberkochen, Germany). An excitation wavelength of 633 nm was used to visualize FM4-64 staining, and the germinated

ascospores were examined using 100x or 63x objectives. Three-dimensional images were constructed from three or more optical slices of one µm or smaller (Zeiss LSM Image Browser, Carl Zeiss, Oberkochen, Germany). The incorporation of FM4-64 into membrane-bound components of the endocytic system was evaluated over time. The first images were taken immediately after stain application and then were captured at 30-s intervals through 30 min. A control treatment included ascospores germinated in MM alone before staining with FM4-64.

Influence of inhibitory peptide f3-16 on sterol-rich membrane domain distribution and cell-wall chitin deposition. Ascospores of *G. zeae* were collected and prepared in the same manner as for staining of the endocytic system. After incubation in 0.2 µM f3-16 for 18 h, germinated ascospores were stained with filipin III (Cayman Chemical, Ann Arbor, MI) to visualize SRDs. Germinated ascospores were immersed 700 µl of MM containing 15 µg ml^{-1} filipin and incubated for 10 min. Excess stain was removed by 3 washes with MM, and a cover slip was placed over the spores. The plasma membrane of stained germinated ascospores was visualized at least 30 min after filipin application using laser-scanning confocal microscopy. An excitation wavelength of 405 nm was used to visualize filipin staining, and germinated ascospores were examined using 100x or 63x objective. Three-dimensional images were constructed from three or more optical slices of one µm or smaller ().

Germinated ascospores were also stained with WGA:AlexaFluor 594 (Molecular Probes, Invitrogen Corporation, Carlsbad, California) to visualize the pattern chitin synthesis. After incubation for 18 h in 0.2 µM f3-16, germinated ascospores were immersed in 700 µl of MM containing 5 µg ml^{-1} WGA and incubated for 2 min. Excess

stain was removed with 3 washes of MM, and a cover slip was placed over the spores. The cell walls of WGA-stained ascospore germlings were visualized at least 30 min after staining. An excitation wavelength of 543 nm was used to visualize WGA staining, and the germinated ascospores were examined using 100x or 63x objectives. Three-dimensional images were constructed from three or more optical slices of one μm or smaller ().

A control treatment included ascospores germinated in MM alone before staining with either filipin or WGA.

RESULTS

Effects of inhibitory peptide f3-16 on structural components of the endocytic system. Germination of ascospores incubated in MM typically began after four h. After 18 h germ-tubes had adhered to the bottom of WilCo Dishes and were stained and observed. Within 3 min of FM4-64 application, the germ-tube plasma membrane became visible (Table 1, Fig. 1A). The plasma membranes of non-germinated cells of the ascsospores were also stained by this time. Between 3 to 5 min, the plasma membranes associated with septal walls of the germ-tube became visible (Fig. 1B). By 4 or 5 min, small structures, typical of endocytic vesicles, became visible (Fig. 1C). These endosomes were punctate and adhered to the plasma membrane of all germ-tube cells. They were also visible in non-germinated ascospore cells where they were adhered to the plasma membrane (Fig. 1C). Within 5 to 6 min of stain application, punctate structures began to accumulate within the cytoplasm. These appeared to be mobile because their distribution changed over time during observation using real-time imaging (Fig. 1C).

Shortly after the appearance of cytoplasmic punctate structures, large oblong vacuoles became visible in the cytoplasm (arrow, Fig. 1D). Each germ-tube cell ultimately contained 1 to 3 of these vacuoles that filled most of the cytoplasm. Finally, staining of the Spitzenkörper in the apical germ-tube cell occurred 6 to 7 min after stain application (arrowhead, Fig 1E). No further changes in structural components of the endocytic system within germ-tube cells were noted through 30 min of observation.

When incubated in 0.2 μM f3-16, ascospores began to germinate after 6 h and, after an overnight incubation in MM, possessed germ-tubes that were shorter and wider in diameter than non-treated ascospores (Fig. 2). When stained with FM4-64, the plasma membrane, septum-associated plasma membrane, and endocytic vesicles became visible within a similar timeframe as in ascospores incubated in MM. After 5 to 6 minutes, early endosomes densely accumulated within the cytoplasm of all germ-tube cells (Fig. 2). However, in contrast to ascospores incubated only in MM, the large vacuoles were not observed in germ-tube cells through 30 min. Commonly a large, round vacuole would be observed at the polar tip of the germ-tube apex (arrowhead, Fig. 2B). Through 30 min of observation the Spitzenkörpers were not stained sufficiently to visualize.

TABLE 1. FM4-64 staining of stuctural components of the endocytic system of germinated *Gibberella zeae* ascospores incubated in minimal medium[a]

Time after staining (min)	Origin of FM4-64 fluorescence
< 3	- Plasma membrane
3 – 5	- Septum-associated plasma membrane
4 – 5	- Small, punctate structures adhered to plasma membrane of all germ-tube cells
	- Small, punctate structures adhered to plasma membrane of all non-germinated ascospore cells
5 – 6	- Small, spherical vesicles distributed throughout the cytoplasm of germ-tube cells
	- Large, oblong vacuoles in germ-tube cells
	- Single, large vacuole in each non-germinated ascospore cell
6 – 7	- Spitzenkörper

[a] Ascospores were incubated in mimimal medium (MM) (ref) in the dark for 18 h at 24˚C. Images were captured at 30-s intervals beginning immediately after FM4-64 application.

TABLE 2. FM4-64 staining of structural components of the endocytic system of germinated *Gibberella zeae* ascospores incubated in inhibitory peptide[a]

Time after staining (min)	Origin of FM4-64 fluorescence
< 3	- Plasma membrane
3 – 5	- Septum-associated plasma membrane
4 – 5	- Small, punctate structures adhered to plasma membrane of all germ-tube cells
5 – 6	- Dense accumulation of small vesicles in the cytoplasm of all germ-tube cells
	- Multiple vacuoles in non-germinated ascospore cells
< 30	- Spitzenkörper not visible

[a] Ascospores were incubated in minimal medium (MM) (ref) amended with 0.2μM f3-16 for 18 h in the dark at 24˚C. Images were captured at 30-s intervals beginning immediately after FM4-64 application.

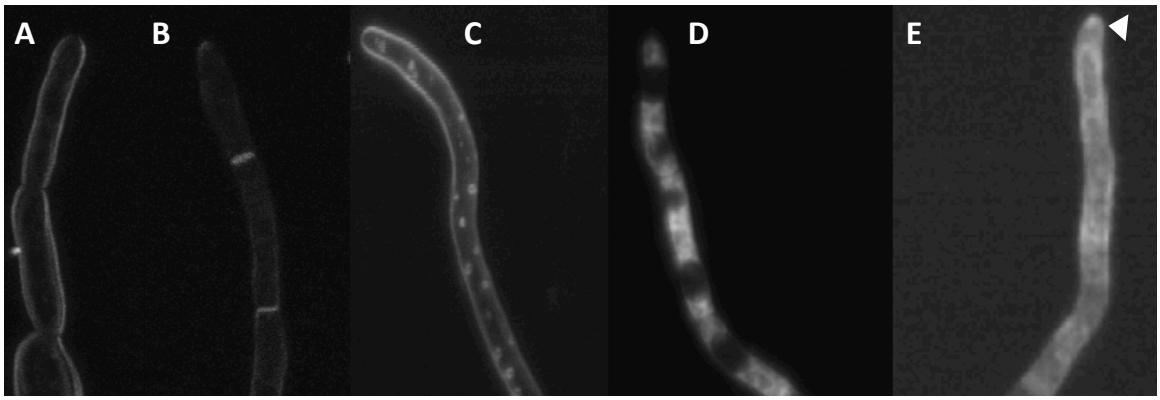

Fig. 1. Germinating *Gibberella zeae* ascospores incubated in minimal medium (27) and stained with FM4-64 to visualize structural components of the endocytic system. Staining of the germ-tube plasma membrane, **A**. Septum-associated plasma membrane, **B**. Endocytic vesicles, adhered to germ-tube plasma membrane, and mobile early endosomes, free in the cytoplasm, **C**. Cytoplasm-filling vacuoles in germ-tube cells, **D**. Spitzenkörper-like structure (arrow), **E**. Bar = 5 μm.

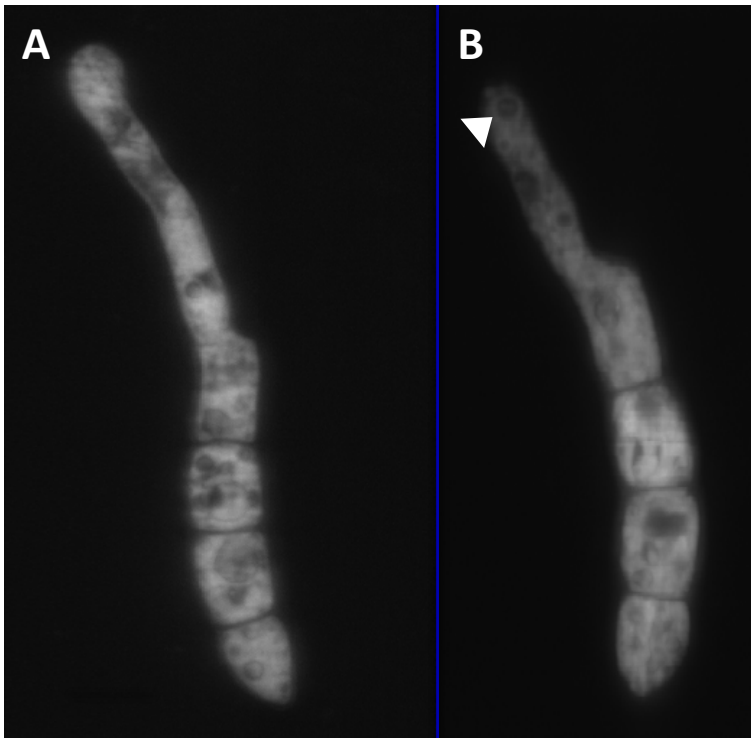

Fig. 2. Germinating *Gibberella zeae* ascospores incubated with 0.2 µM f3-16, then stained with FM4-64. When incubated with f3-16, endosomes accumulated in germ-tubes without the appearance of larger vacuoles when treated with f3-16, **A**. Also, a large, spherical vacuole, located at the polar tip of a germ-tube apical cell was commonly observed (arrow), **B**. Brackets indicate germ-tubes. Bar = 5 µm.

Influence of inhibitory peptide f3-16 on sterol-rich membrane domain distribution and cell-wall chitin deposition. Germination of ascospores incubated in MM typically began after four h. After 18 h, germ-tubes had adhered to the bottom of WilCo Dishes and were stained and observed. When incubated in MM, membrane regions rich in sterols were stained strongly by filipin at the apex of the germ-tube (Fig. 3A). Additional strongly stained membranes were visible at septation sites and locations of lateral branch formation (not shown).

Patterns of sterol-rich membrane regions differed in germinated ascospores incubated with peptide 0.2 μM f3-16. In this treatment, sterol-rich regions were not strongly stained at the germ-tube apex, but they were evident in association with septa (not shown). In addition, SRDs were distributed sub-apically along the germ-tube (Fig. 3B).

Patterns of chitin synthesis also differed in ascospores incubated in 0.2 μM f3-16 for 18 h. In germinated ascospores of *G. zeae* incubated in MM, the germ-tube apex and septa were most strongly stained with WGA (Fig. 4A). The remainder of the germ-tube was dimly fluorescent.

When chitin was visualized in germinated ascospores incubated in 0.2 μM f3-16, brightly staining apical regions of germ-tubes were not noticeable (Fig. 4B). Additionally, cell-wall chitin was unevenly stained along the remaining length of the germ-tube (Fig. 4B).

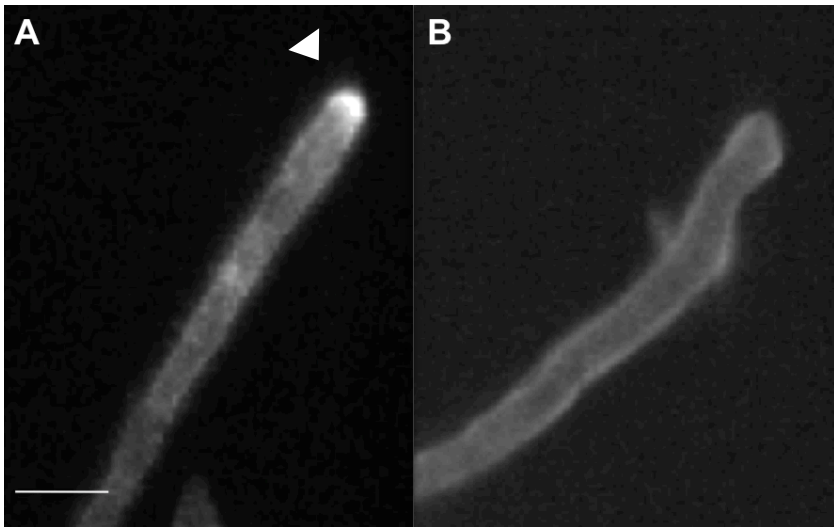

Fig. 3. Germinating *Gibberella zeae* ascospores incubated in minimal medium (27) or 0.2 μM f3-16, for 18 h, then stained with filipin to visualize sterol-rich domains in plasma membranes. Brightly staining polar tip of germ-tube apical cell incubated in MM, **A.** Lack of concentrated staining of polar tips of germ-tube apical cells and uneven staining of sub-apical plasma in germ-tube incubated in f3-16, **B**. Bar = 5 μm.

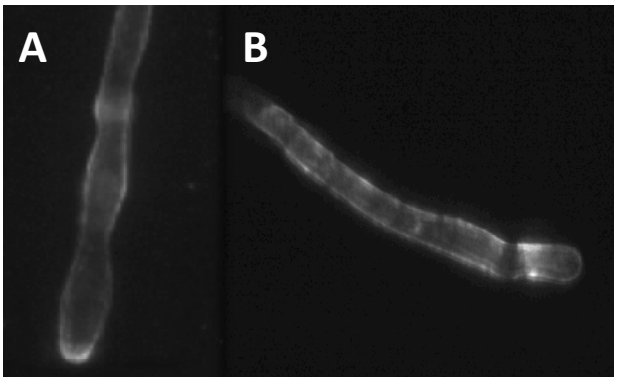

Fig 4. Germinating *Gibberella zeae* ascospores incubated in minimal medium, **A**, or 0.2 μM f3-16, **B**, for 18 h, then stained with wheat-germ agglutinin to visualize cell-wall chitin. Brightly staining polar tips of apical germ-tube cells, **A**. Uneven and sub-apical WGA staining of germ-tube cells, **C**. Bar = 5 μm

DISCUSSION

These studies have established that the inhibitory peptide f3-16 induces modifications in the patterns of endocytosis, the distribution of plasma-membrane sterol-rich domains, and patterns of cell wall synthesis in germinating *G. zeae* ascospores. Structural modifications in germ-tube cells were effectively visualized by the use of the vital stains FM4-64, filipin, and WGA.

Polar development of germ-tubes depends on the balance between exocytosis and endocytosis. Components of the *G. zeae* endocytic system were initially characterized in ascospores incubated a minimal growth medium. Within minutes after stain application, FM4-64 was incorporated into the plasma membrane of germ-tube cells and septum-associated membranes of all germ-tube cells. Subsequently, stained organelles, resembling endocytic vesicles developed adjacent to the plasma membrane. With additional time these vesicles disassociated from the membrane. Mobile organelles resembling endosomes then appeared throughout the cytoplasm. Eventually endosomes in sub-apical cells became less visible as large, cytoplasm-filling vacuoles began to accumulate. Finally, as endosomes and vacuoles appear, the Spizenkörper also became visible.

The pattern of endocytic component staining in *G. zeae* resembled patterns previously described in *A. nidulans* (33)*, Aspergillus oryzae* (25)*, M. grisea* (3)*, N. crassa* (45)*,* and *Ustilago maydis* (39). The timing of component staining, however, has been characterized only in *M. grisea.* The timing of component staining in that fungal species differed from that of *G. zeae.* Staining of all endocytic components in *M. griesa* occurred in 45 minutes, in contrast to only 10 minutes required for endocytic component staining

in *G. zeae.* Differences in the timing of component staining may be related to differing stages of spore germination and growth between the two organisms. In the case of germinating conidia of *M. grisea,* stain was applied shortly after a germ-tube had emergered and consisted of a single cell. In the case of *G. zeae*, the ascospore germ-tubes were composed of 3 to 4 cells. At the time of staining, it is possible that germ-tubes of the two fungi differed with respect to metabolic rate that could affect the rates of exocytosis and endocytosis.

When ascospores were treated with peptide f3-16, the staining of the endocytic system components was initially similar to staining of germ-tubes incubated in a minimal growth medium. Plasma membrane, septum-associated membranes, endocytic vesicles, and endosomes were clearly visible within a similar time frame. However, over time endosome-like organelles continued to accumulate, but vacuoles did not dominate the cytoplasm of subapical cells. Endosomes filled much of the cytoplasm and through 30 minutes of observation, no structure resembling a Spitzenkörper was stained. Instead, a spherical vesicle, larger than endosomes, was usually located at the polar tip of the apical germ-tube cell.

As has been reported by Cheng, et al. (14) and Rittenour, et al. (36), SRDs were noted predominately at the polar tip of the apical germ-tube cells incubated in a minimal growth medium. These domains also were concentrated at the sites of septum formation.

In contrast, when *G. zeae* ascospores were incubated with peptide f3-16, SRDs were not localized to the polar tip of the apical cell nor at points or septation. Instead, SRDs were distributed sub-apically along the germ-tube length.

Pearson et al. established the importance of actin filament anchoring to SRDs for polarized growth in *A. nidulans.* In mutant isolets, the investigators identified MesA, as a SRD-associated protein required for actin filament anchoring, and the establishment and maintenance of polarity. Whether the modifications of SRD distribution in *G. zeae,* treated with peptide f3-16 also disrupt the normal patterns of actin filament anchoring leading to aberrant growth is uncertain and requires further study.

When incubated in a minimal growth medium, chitin staining was most prominent at the polar tip of the apical germ-tube cell, at branch points, and at septa. In more mature regions of cell wall, chitin staining was minimal. This pattern of chitin staining was similar to that reported in *A. nidulans* (24).

The pattern of chitin deposition was modified when ascospores were incubated with peptide f3-16. In these germ-tubes, patchy regions of chitin were prominently stained behind the polar tip of the germ-tube apical cell, while the polar tip itself was not prominently stained.

Modified chitin distribution in peptide-treated germ-tubes could be caused by incomplete vacuole formation or inhibition of vesicle trafficking. Improper chitin synthase localization or enzyme turnover may contribute to the patchy distributions of chitin behind the polar tip, as suggested in *A. oryazae* (25). Chitin-synthase localization studies will help to clarify the basis of modified chitin distribution patterns in relation to peptide f3-16 exposure.

Cytological phenotypes observed in the present study will be useful for investigations of mechanisms by which germ-tube cells respond to inhibitory peptides,

such as f3-16. This study provides a focus for future experiments, which could utilize additional molecular markers for structural, signaling, and synthetic components of *G. zeae* cells.

Literature Cited

1. Abenza, J. F., Pantazopolou, A., Rodríguez, J. M., Galindo, A., and Peñalva, M. A. 2009. Long-distance movement of *Aspergillus nidulans* early endosomes on microtubule tracks. Traffic 10:57-79.
2. Alverez, F. J, Douglas, L. M., and Konopka, J. B. 2007. Sterol-rich plasma membrane domains in fungi. Eukaryot. Cell. 6:755-763.
3. Atkinson, H. A., Daniels, A., and Read, N. D. 2002. Live-cell imaging of endocytosis during conidial germination in the rice blast fungus *Magnaporthe grisea.* Fungal Genet. Biol. 37:233-244
4. Beyer, M. and Verreet, J-A. 2005. Germination of *Gibberella zeae* ascospores as affected by age of spores after discharge and environmental factors. Eur. J. Plant Pathol. 111:381-389.
5. Beyer, M., Verreet, J-A., and Ragab, W. S. M. 2005. Effect of relative humidity on germination of ascospores and macroconidia of *Gibberella zeae* and deoxynivalenol production. Int. J. Food. Microbiol. 98:233-240.
6. Bishop-Hurley, S. L., Mounter, S. A., Laskey, J., Morris, R. O., Elder, J, Roop, P., Rouse, C., Schmidt, F. J., and English, J. T. 2002. Phage-displayed peptides as developmental agonists for *Phytophthora capsici* zoospores. App. Environ. Mircrobiol. 68:3315-3320.
7. Bishop-Hurley, S. L., Schmidt, F. J., Erwin, A. L., Smith, A. L. 2005. Peptides selected for binding to a virulent strain of *Haemophilus influenzae* by phage display are bactericidal. Antimicrob. Agents Chemother. 49:2972-2978.

8. Blondelle, S. E. and Lohner, K. 2000. Combinatorial libraries: a tool to design antimicrobial and antifungal peptide analogues having lytic specificities for structure-activity relationship studies. Biopolym. Pept. Sci. 55:74-87.
9. Bolte, S., Talbot, C., Boutte, Y., Catrice, O., Read, N. D., and Satiat-Jeunemaitre, B. 2004. FM-dyes as experimental probes for dissecting vesicle trafficking in living plant cells. J. Microsc. (Oxf.). 214:159-173.
10. Bowman, S. M. and Free, S. J. 2006. Review: The structure and synthesis of the fungal cell wall. BioEssays 28:799-808.
11. Breakspear, A., Pasquali, M., Broz, K., Dong, Y., and Kistler, C. 2011. *Npc1* is involved in sterol trafficking in the filamentous fungus *Fusarium graminearum.* Fungal Genet. Biol. 48:725-730.
12. Cabib, E. The synthesis and degradation of chitin. Adv. Enzymol. 59:59-101.
13. Catanzariti, A-M., Dodds, P. N., Lawrence, G. J., Ayliffe, M. A., and Ellis, J. G. 2006. Haustorially expressed secreted proteins from flax rust are highly enriched for avirulence elicitors. The Plant Cell 18:243-256.
14. Cheng, J., Park, T-S., Fischl, A. S., and Ye, X. S. 2001. Cell cycle progression and cell polarity require sphingolipid biosynthesis in *Aspergillus nidulans*. Mol. Cell Biol. 21:6198-6209.
15. Fang, Z. D., Laskey, J. G., Huang, S., Bilyeu, K. D., Morris, R. O., Schmidt, F. J., and English, J. T. 2006. Combinatorially selected defense peptides protect plant roots from pathogen infection. Proc. Natl. Acad. Sci. USA. 103:18444-18449

16. Fang, Z. D., Marois, J. J., Stacey, G., Schoelz, J. E., English, J. T., and Schmidt, F. J. 2010. Combinatorially selected peptides for protection of soybean against *Phakopsora pachyrhizi*. Phytopathology 100:1111-1117.
17. Fernando, W. G. D., Miller, J. D., Seaman, W. L., Seifert, K., and Paulitz, T. C. 2000. Daily and seasonal dynamics of airborne spores of *Fusarium graminearum* and other *Fusarium* species sampled over wheat plots. Can. J. Bot. 78:497-505.
18. Flor-Parra, I., Sastillo-Lluva, S., and Pérez- Martin, J. 2007. Polar growth in the infectious hyphae of the phytopathogen *Ustilago maydis* depends on a virulence-speciic cyclin. The Plant Cell. 19:3280-3296.
19. Gallagher, J. T., Morris, A., Dexter, T.M. 1985. Identification of two binding sites for wheat-germ agglutinin on polylactosamine-type oligosaccharides. Biochem. J. 231:115-122.
20. Goswami, R. S., and Kistler, H. C. 2004. Pathogen profile: Heading for disaster: *Fusarium graminearum* on cereal crops. Mol. Plant. Pathol. 5:515-525.
21. Guenther, J. C. and Trail, F. 2005. The development and differentiation of *Gibberella zeae* (anamorph: *Fusarium graminearum*) during colonization of wheat. Mycologia. 97:229-237.
22. Harris, S. D. 2005. Morphogenesis in germinating *Fusarium graminearum* macroconidia. Mycologia. 97:880-887.
23. Harris, S. D., Read, N. D., Roberson, R. W., Shaw, B., Seiler, S., Pamann, M. and Momany, M. 2005. Minireview: Polarisome meets Spitzenkörper: microscopy, genetics, and genomics converge. Eukaryot. Cell. 4:225-229.

24. Harris, S. D., Hofmann, A. F., Tedford, H. W., and Lee, M. P. 1999. Identification and characterization of genes required for hyphal morphogenesis in the filamentous fungus *Aspergillus nidulans.* Genetics. 151:1015-1025.

25. Higuchi, Y., Arioka, M., and Kitamoto, K. 2009. Endocytic recycling at the tip region in the filamentous fungus *Aspergillus oryzae.* Commun. Integr. Biol. 2:327-328.

26. Hill, D. F., Pertersen, G. B. 1982. Nucleotide sequence of bacteriophage f1 DNA. J. Virol. 44:32-46.

27. Hoffmann, J. and Mendgen, K. 1998. Endocytosis and membrane turnover in the germ tube of *Uromyces fabae.* Fungal Genet. Biol. 24:77-85.

28. Marcos, J. F., Muñuz, A., Pérez-Payá, E., Misra, S., and López-García, B. 2008. Identification and rational design of novel antimicrobial peptides for plant protection. Annu. Rev. Phytopathol. 46:273-301.

29. Klittich, C. J. R. and Leslie, J. F. 1988. Nitrate reduction mutants of *Fusarium moniliforme* (*Gibberella fujikuroi*). Genetics 118:417-423.

30. Lipke, P. N. and Ovalle, R. 1998. Minireview. Cell wall architecture in yeast: new structure and new challenges. J. Bacteriol. 180:3735-3740.

31. Müller, O., Schreier, P. H., and Uhrig, J. F. 2008. Identification and characterization of secreted and pathogenesis-related proteins in *Ustilago maydis.* Mol. Genet. Gen. 279:27-39.

32. Nesher, I., Minz, A., Kokkelink, L., Trdzyski, P., and Sharon, A. 2011. Regulation of pathogenic spore germination by CgRac1 in the fngal plant pathogen *Colletotrichum gloeosporioides.* Eukaryot. Cell. 10:1122-1130.

33. Peñalva, M. A. 2005. Tracing the endocytic pathway of *Aspergillus nidulans* with FM4-64. Fungal. Genet. Biol. 42:963-975.

34. Petrenko, V. A., Smith, G. P., Gong, X. and Quinn, T. 1996. A library of organic landscapes on filamentous phage. Protein Eng. 9:797-801.

35. Reynaga-Peña, C. G., Cierz, G., and Bartinicki-Garcia, S. 1997. Analysis of the role of the Spitzenkörper in fungal morphogenesis by computer simulation of apical branching in *Aspergillus niger.* Proc. Natl. Acad. Sci. USA. 94:9096-9101.

36. Rittenour, W. R., Chen, M., Cahoon, E. B., and Harris, S. D. 2011. Control of glucosylceramide production and morphogenesis by the Bar1 Ceramide Synthase in *Fusarium graminearum.* PLoS One. 6:e19385.

37. Rittenour, W. R. and Harris, S. D. 2008. Characterization of *Fusarium graminearum* Mes1 reveals roles in cell-surface organization and virulence. Fungal Genet. biol. 45:933-946.

38. Roncero, C., and Durán, A. 1985. Effect of calcofluor white and congo red of fungal cell wall morphogenesis: in vivo activation of chitin polymerization. J. Bacteriol. 163:1180-1185.

39. Seong, K-Y., Zhao, X., Xu, J-R., Güldener, U., and Kistler, H. C. 2008. Conidial germinaiton in the filamentous fungus *Fusarium graminearum.* Fungal Genet. Biol. 45:389-399.

40. Shoji, J., Ariolka, M., Kitamoto, K. 2008. Dissecting cellular components of the secretory pathway in filamentous fungi: insights into their application or protein production. Biotechnol. lett. 30:7-14.

41. Siafakas, A. R., Wright, L. C., Sorrell, T. C., and Djordjevic, J. T. 2006. Lipid rafts in *Cryptococcus neoformans* concentrate the virulence determinants Phospholipase B1 and Cu/Zn Superoxide Dismutase. Eukaryot. Cell. 5:488-498.

42. Smith, G. P. and Petrenko, V. A. 1997. Phage Display. Chem. Rev. 97:391-410.

43. Steinberg, G. 2007. On the move: endosomes in fungal growth and pathogenicity. Nature Rev. Microbiol. 5:309-316.

44. Sudbery, P. 2011. Review: Fluorescent proteins illuminate the structure and function of the hyphal tip apparatus. Fungal Genet. Biol. 48:849-857.

45. Trail, F., Common, R. 2000. Perithecial development by *Gibberella zeae:* a light microscopy study. Mycologia 92:130–138.

46. Upadhyay, S. and Shaw, B. D. 2008. The role of actin, fimbrin and endocytosis in growth of hyphae in *Aspergillus nidulans.* Mol. Microbiol. 68:690-705.

47. Veses, V., Richards, A., Gow, A. R. 2008. Vacuoles and fungal biology. Curr. Opin. Microbiol. 11:503-510.

48. Watters, M. K., Humphries, C., De Vries, I., and Griffiths, A. J. F. 2000. A homeostatic set point for branching in *Neurospora crassa*. Mycol. Res. 104:557-563.

49. Watters, M. K., Virag, A., Haynes, J., and Griffiths, A. J. F. 2000. Branch initiation in *Neurospora* is influenced by events at the previous branch. Mycol. Res. 104:805-809.

50. Xu, X-M., Monger, W., Ritieni, A., and Nicholson, P. 2007. Effect of temperature and duration of wetness during initial infection periods on disease

development, fungal biomass and mycotoxin concentrations on wheat inoculated with single, or combinations of, *Fusarium* species. Plant Pathol. 56:943-956.

51. Yu, J. and Smith, G. P. 1996. Affinity maturation of phage-displayed peptide ligands. Methods Enzymol. 267:3-27.